

UC Irvine

UC Irvine Previously Published Works

Title

Influence of southern hemispheric biomass burning on midtropospheric distributions of nonmethane hydrocarbons and selected halocarbons over the remote South Pacific

Permalink

<https://escholarship.org/uc/item/94v18766>

Journal

Journal of Geophysical Research Atmospheres, 104(D13)

ISSN

0148-0227

Authors

Blake, NJ
Blake, DR
Wingenter, OW
[et al.](#)

Publication Date

1999-07-20

DOI

10.1029/1999JD900067

Copyright Information

This work is made available under the terms of a Creative Commons Attribution License, available at <https://creativecommons.org/licenses/by/4.0/>

Peer reviewed

Influence of southern hemispheric biomass burning on midtropospheric distributions of nonmethane hydrocarbons and selected halocarbons over the remote South Pacific.

Nicola J. Blake¹, Donald R. Blake¹, Oliver W. Wingenter^{1,2}, Barkley C. Sive¹, Lisa M. McKenzie¹, Jimena P. Lopez¹, Isobel J. Simpson¹, Henry E. Fuelberg³, Glen W. Sachse⁴, Bruce E. Anderson⁴, Gerald L. Gregory⁴, Mary Anne Carroll⁵, George M. Albercook⁵, and F. Sherwood Rowland¹

Abstract. Aircraft measurements of nonmethane hydrocarbons (NMHCs) and halocarbons were made over the remote South Pacific Ocean during late August-early October 1996 for NASA's Global Tropospheric Experiment (GTE) Pacific Exploratory Mission-Tropics A (PEM-Tropics A). This paper discusses the large-scale spatial distributions of selected trace gases encountered during PEM-Tropics A. The PEM-Tropics A observations are compared to measurements made over the southwestern Pacific in early November 1995 as part of Aerosol Characterization Experiment (ACE 1). Continental pollution in the form of layers containing elevated levels of O₃ was observed during a majority of PEM-Tropics flights, as well as during several ACE 1 flights. The chemical composition of these air masses indicates that they were not fresh and were derived from nonurban combustion sources. The substantial impact of biomass burning on the vertical structure of the South Pacific troposphere is discussed.

1. Introduction

Biomass burning has been recognized recently as a major source of important trace gases, including carbon dioxide (CO₂), carbon monoxide (CO), methane (CH₄), nonmethane hydrocarbons (NMHCs), methyl chloride (CH₃Cl), and methyl bromide (CH₃Br) [Crutzen and Andreae, 1990; Levine, 1991, 1996; Blake *et al.*, 1996b]. The term includes the extensive burning of natural grasslands and savannas, to sustain nomadic agriculture, and the disposal of agricultural wastes. Biomass burning is also associated with deforestation, slash and burn agriculture, forest wildfires, and wood used as fuel for cooking and heating [e.g., Seiler and Crutzen, 1980; Logan *et al.*, 1981; Levine, 1991]. Most of these activities are controlled by humans, and the emissions from the burning of biomass represent a large perturbation to global atmospheric chemistry, especially in the tropics where most of the combustion takes place [Andreae, 1991].

A principal goal of PEM-Tropics A was to investigate the impact of distant human activity on the remote south central Pacific troposphere. The overall scientific rationale and

description of individual aircraft missions is given in the PEM-Tropics A overview paper [Hoell *et al.*, 1999]. The timing of the experiment corresponded to the end of the dry season in many regions of the Southern Hemisphere, when southern Africa, South America, Australia, and Indonesia are sites of widespread biomass burning [e.g., Andreae, 1991; Hao and Liu, 1994; Hurst *et al.*, 1994; Fishman *et al.*, 1996; Justice *et al.*, 1996; Connors *et al.*, 1996]. Satellite observations in the 1980s revealed that the Southern Hemisphere troposphere is dominated during the austral spring by an ozone (O₃) maximum stretching over two thirds of the latitudinal band from South America across the South Atlantic and Indian Oceans into the southwestern Pacific [Fishman *et al.*, 1990]. Work is in progress to characterize the yearly frequency of fires in the different biomass burning regions, their localization, and the size of burn areas [e.g., Olson *et al.*, 1999].

Matsueda *et al.* [1998] reported a strong seasonal maximum in CO mixing ratios in the upper troposphere over the western Pacific in the latitude range 20°–30°S during October and November 1994 and 1995. Air mass back trajectories for these enhancements indicate that CO-rich air from biomass burning in South America and/or southern Africa was injected into the free troposphere by convection and rapidly transported over the Indian Ocean into the western Pacific.

This paper describes the large-scale spatial distribution of selected NMHCs, CH₃Cl, tetrachloroethene (C₂Cl₄), O₃, and CO over the South Pacific during PEM-Tropics A. Comparisons are drawn between similar measurements over the South Pacific during the Aerosol Characterization Experiment (ACE 1) conducted in early November 1995. The impact of biomass burning plumes on the vertical distribution of the trace gases and O₃ is discussed.

¹Department of Chemistry, University of California, Irvine.

²Now at School of Earth and Atmospheric Sciences, Georgia Institute of Technology, Atlanta.

³Department of Meteorology, Florida State University, Tallahassee.

⁴NASA Langley Research Center, Hampton, Virginia.

⁵Atmospheric, Oceanic and Space Sciences, University of Michigan, Ann Arbor.

2. Experiment

PEM-Tropics A employed two aircraft, the NASA Ames DC-8 and the NASA Wallops P-3B, and took place between August 24 and October 6, 1996. The payloads of both aircraft included instruments capable of quantifying an extensive suite of atmospheric species, including NMHCs, CH_3Cl , C_2Cl_4 , alkyl nitrates (RONO_2), CO , O_3 , NO_x , peroxyacetyl nitrate (PAN), nitric acid (HNO_3), and aerosols [Hoell *et al.*, 1999]. The two aircraft sampled an area of the Pacific stretching from northeast of Hawaii to the tip of Antarctica (45.2°N – 72.5°S), and northwest of Fiji to the west coast of South America (152.7°E – 78.0°W) (Plate 1). The scientific payloads of the two aircraft differed in some respects, reflecting the operating characteristics of the two platforms. The high-altitude ceiling (typical altitude range 0.3–11.9 km during PEM-Tropics A) and long range of the DC-8 favored the extensive geographical survey of the South Pacific troposphere, a region for which few trace gas data were available previously. By contrast, the low-altitude capabilities of the P-3B (typical altitude range 0.06–8.5 km during PEM-Tropics A) allowed detailed characterization of Marine Boundary Layer (MBL) processes.

As part of the International Global Atmospheric Chemistry (IGAC) project First Aerosol Characterization Experiment (ACE 1), the National Center for Atmospheric Research (NCAR) C-130 aircraft flew an extended latitudinal survey between 76°N and 60°S through the center of the Pacific basin during early November 1995 (Plate 1). A maximum flight altitude of 6.2 km was attained by the NCAR C-130 in the Southern Hemisphere during this series of southbound transit flights.

The University of California, Irvine (UCI), group collected whole air samples aboard the three aircraft during PEM-Tropics A and ACE 1 using procedures described by Blake *et al.* [1992, 1994]. The gas chromatographic analytical apparatus employed after the samples were returned to UCI is described by Blake *et al.* [1996a], Sive [1998], and B. C. Sive *et al.* (manuscript in preparation, 1999 (hereinafter referred to as S99)). Both operations are summarized below.

Aboard the aircraft, a metal bellows pump was used to fill evacuated sample canisters to a pressure of 40 psi. At the UCI laboratory, a 1520 cm^3 (STP) aliquot from each canister was preconcentrated cryogenically in a sample loop. Hydrogen carrier gas flushed the contents of the loop to a splitter, which partitioned and directed the sample flow to five gas chromatographic columns in a reproducible manner. Selected C_1 – C_2 halocarbons were separated by a 60 m, 0.25 mm ID DB-1 column with a 1 μm film thickness (J&W Scientific) and detected with an electron capture detector (ECD). A portion of the effluent from this column was directed to a flame ionization detector (FID) for the detection of selected C_3 – C_{10} NMHCs. The light NMHCs (C_2 – C_5) were analyzed using a 50 m, 0.32 mm ID $\text{Al}_2\text{O}_3/\text{Na}_2\text{SO}_4$ PLOT column (Chrompack) coupled to an FID. A 60 m, 0.25 mm ID Cyclodex-B column, film thickness 0.25 μm (J&W Scientific), and FID combination separated selected C_6 – C_{10} NMHCs. An ECD detector and a 60 m, 0.25 mm ID DB-5MS column, film thickness 0.5 μm (J&W Scientific) were used for the analysis of selected C_1 – C_2 halocarbons and methyl nitrate. An ECD and an RTX-1701 column were employed for the determination of C_1 – C_2 halocarbons and C_1 – C_4 alkyl nitrates. The unique separation characteristics of each column were optimal for a particular subset of NMHC or halocarbon gases and, in

combination, provided a comprehensive suite of gas measurements.

The combination of variable detector response and chromatographic factors results in a limit of detection (LOD) for each NMHC of approximately 3 parts per trillion by volume (pptv). The measurement precision was about 1% or 1.5 pptv (1σ), whichever was larger for the alkanes and alkynes, and 3% or 3 pptv (1σ) for the alkenes. The LOD for the halocarbons was variable, but every sample contained each of the reported halocarbons at mixing ratios above their detection limits. The 1σ measurement precision was 2% for CH_3Cl , C_2Cl_4 , and CH_3Br .

The accuracy and precision of the analytical system were closely monitored during the experimental periods according to procedures described by S99. The UCI group has participated in the National Science Foundation sponsored Nonmethane Hydrocarbon Intercomparison Experiment (NOMHICE) overseen by J. Calvert and E. Apel at NCAR [Apel *et al.*, 1994]. Results from NOMHICE demonstrate that our analytical procedures consistently yield accurate identifications of a wide range of unknown hydrocarbons and produce excellent quantitative results [Apel *et al.*, 1994; Sive, 1998; S99].

Fast-response in situ measurements of CO were made spectroscopically using a tunable diode laser instrument during PEM-Tropics A [Sachse *et al.*, 1991] and were made using a gas filter correlation analyzer during ACE 1 [Kok *et al.*, 1998]. In situ O_3 measurements for both PEM-Tropics A and ACE 1 employed $\text{NO}+\text{O}_3$ chemiluminescent detectors (e.g., G. Albercook *et al.*, unpublished data).

The sampling frequencies of the in situ CO and O_3 instruments were much higher than our whole air sampling times during both PEM-Tropics A and ACE 1. We have employed a merged data file generated at Harvard University and containing CO and O_3 mixing ratios averaged over the whole air sampling times for comparison of the different PEM-Tropics A measurement databases. The PEM-Tropics A measurements and merged data files are archived at NASA Langley Research Center and can be accessed via the GTE web site at <http://www-gte.larc.nasa.gov/>. For ACE 1, a merged data set was prepared at UCI. The ACE-1 data archive is maintained by the University Corporation for Atmospheric Research (UCAR) and can be accessed at <http://www.joss.ucar.edu/>.

3. Source Signatures

Tropospheric O_3 has two predominant sources, in situ photochemical production from its precursors (CO , NMHCs, and NO_x) and downward mixing from the stratosphere. When combined with trajectory analysis, the contributions of different precursor sources can be assessed using a wide range of tracers for different source types. Therefore the use of chemical tracers plays a crucial role in establishing the most likely origin of O_3 -enriched layers.

Incomplete combustion is the principal global source of CO , ethane (C_2H_6), and ethyne (C_2H_2). Combustion occurs not only in natural wildfires and in association with land clearing and agricultural land use but also in urban areas through fossil fuel consumption [Andres *et al.*, 1996]. However, some gases such as C_2Cl_4 are specific to industrial/urban activities and serve as markers for such urban

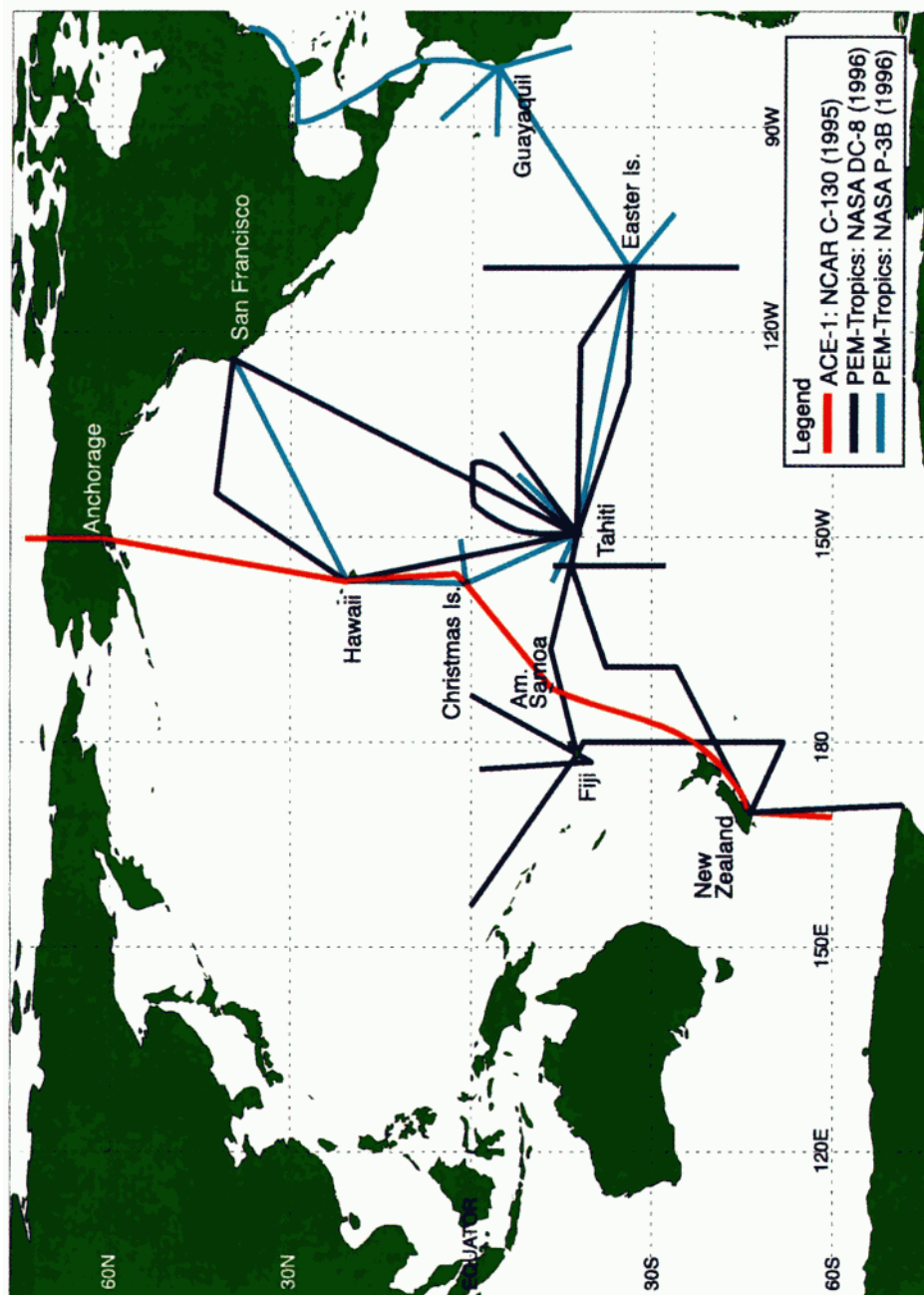


Plate 1. Pacific Exploratory Mission-Tropics A (PEM-Tropics A) DC-8 and P-3B flight tracks (August 24 and October 5, 1996) and Aerosol Characterization Experiment (ACE 1) C-130 southbound transit flight tracks (November 2-13, 1995).

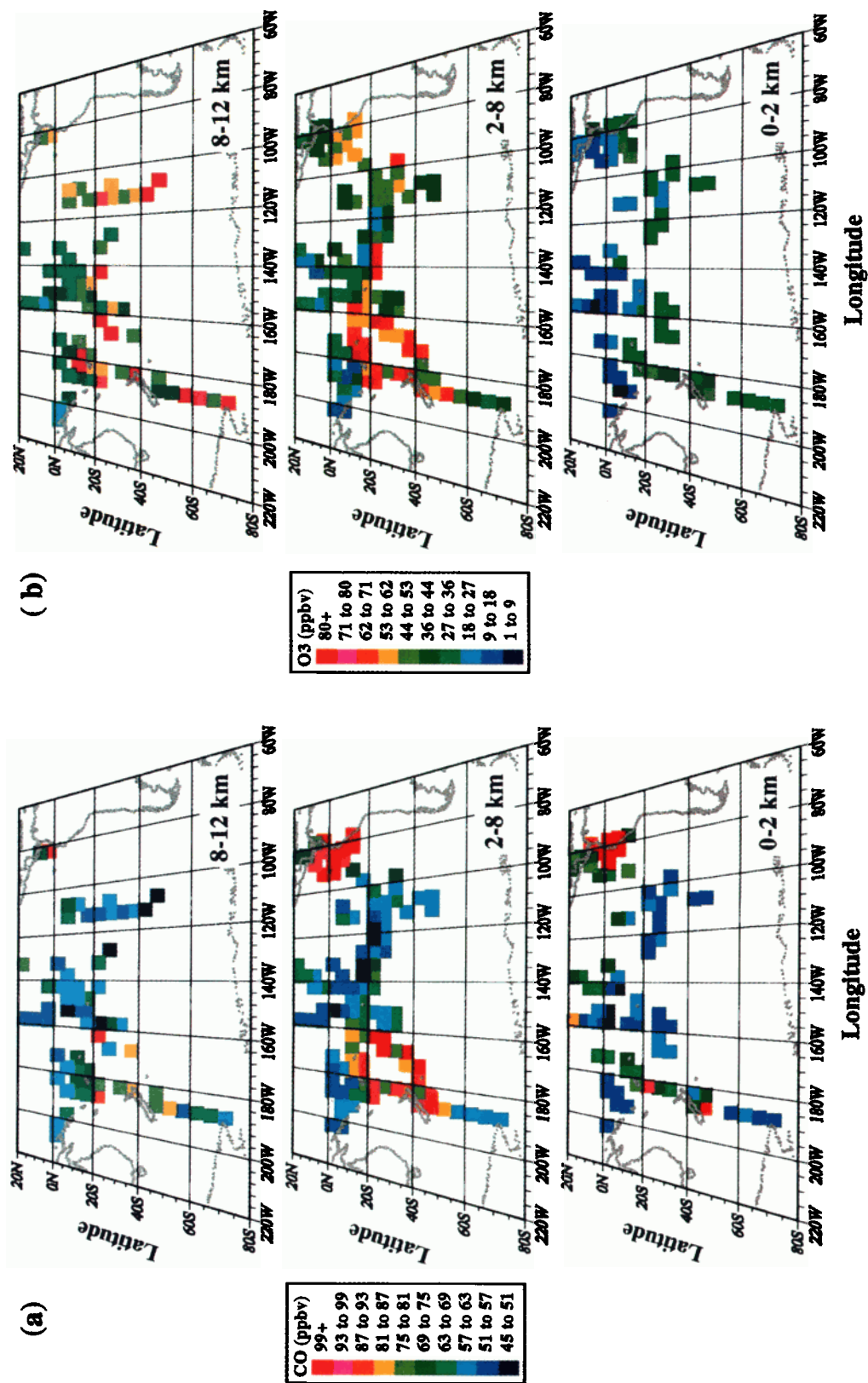


Plate 2. Spatial distribution of (a) CO and (b) O₃ over the Pacific Ocean during PEM-Tropics A for three altitude ranges (0-2, 2-8, and 8-12 km).

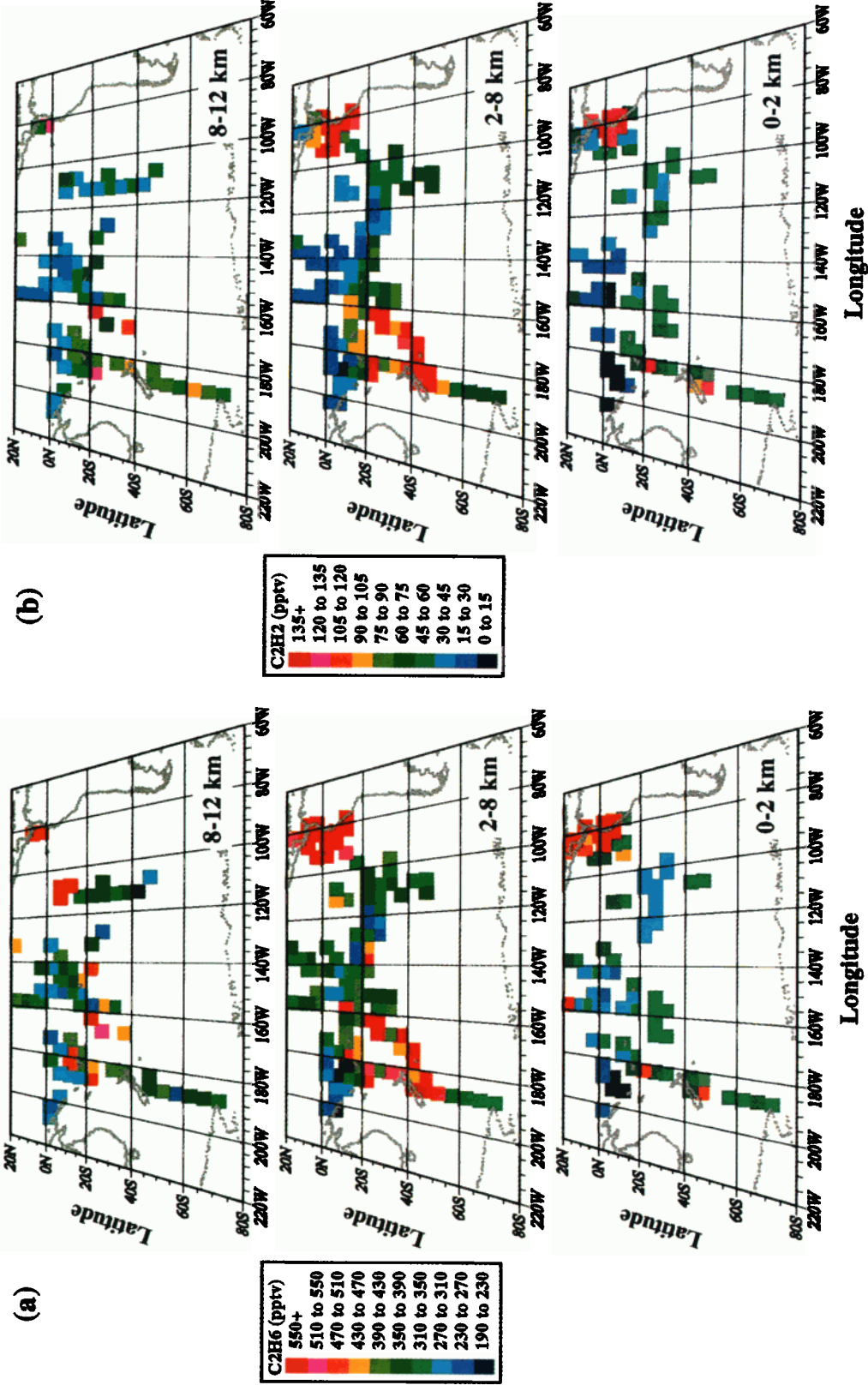


Plate 3. Same as for Plate 2 but for (a) C_2H_6 and (b) C_2H_2 .

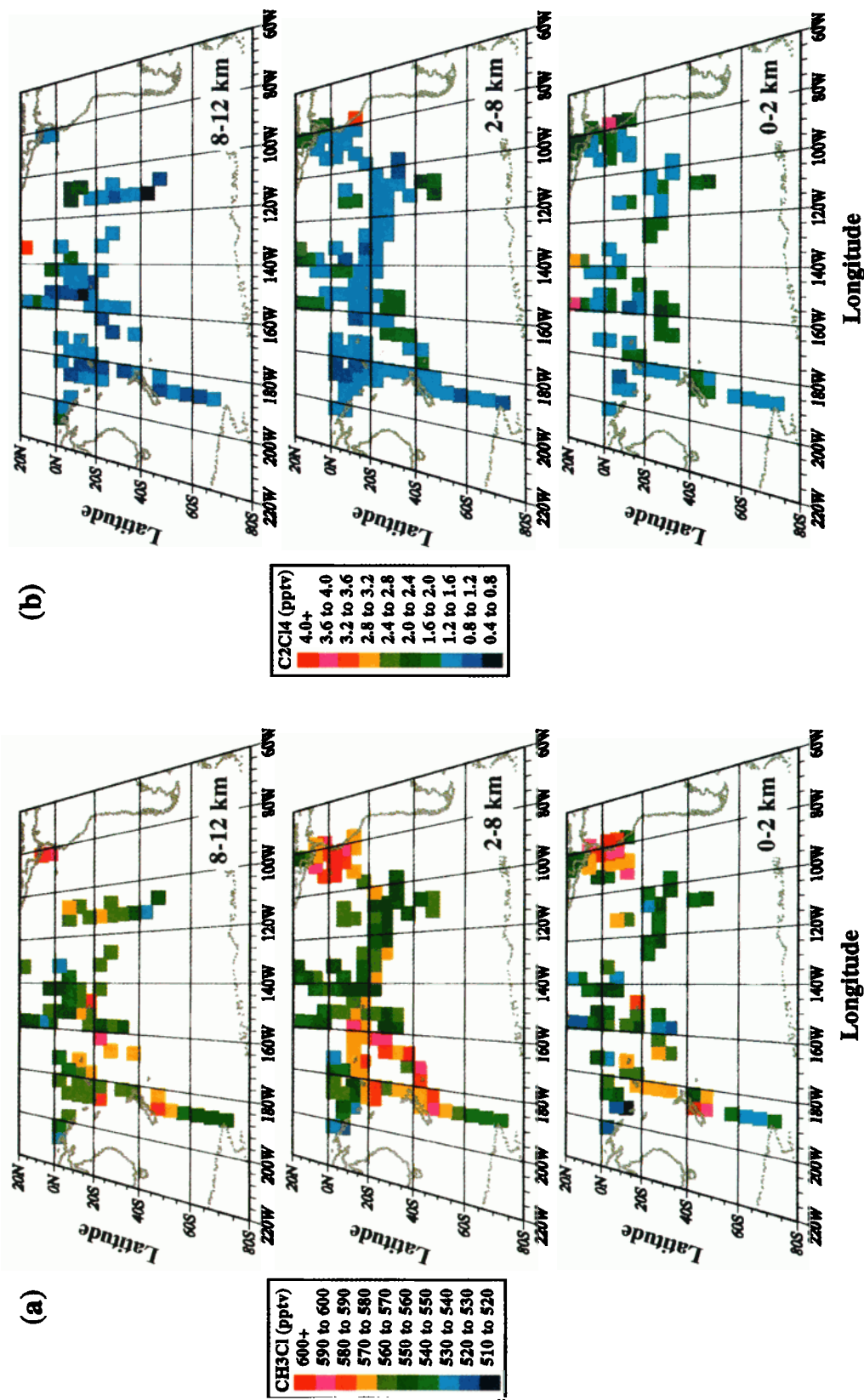


Plate 4. Same as for Plate 2 but for (a) CH₃Cl and (b) C₂Cl₄.

effluents. The majority of C_2Cl_4 (approximately 93%) is emitted in the Northern Hemisphere (P. Midgely, personal communication, 1997). However, enhancements of C_2Cl_4 have been observed downwind of the highly urbanized east coast of Brazil [Talbot *et al.*, 1996] as well as near smaller centers of population visited during PEM-Tropics A (including Guayaquil, Ecuador and Papeete, Tahiti), establishing C_2Cl_4 as a general urban indicator in the Southern as well as in the Northern Hemispheres. Biomass burning is an important global source of CH_3Cl (approximately 25-50%) [e.g., Andreae, 1993; Andreae *et al.*, 1996; Blake *et al.*, 1996b], along with natural production in the surface water of the oceans [Singh *et al.*, 1983]. Mixing ratios of CH_3Cl typically are not elevated in northern cities (i.e., those that do not rely heavily on biomass fuels) [Blake *et al.*, 1997], consistent with CH_3Cl having no significant urban/industrial origins. This makes CH_3Cl a particularly useful diagnostic for biomass burning emissions.

4. Spatial Distributions

Plates 2-4 are color patch plots showing the latitudinal and longitudinal distribution of the mixing ratios of CO , O_3 , C_2H_6 , C_2H_2 , CH_3Cl , and C_2Cl_4 for PEM-Tropics A. The data were averaged over a latitude-longitude grid size of 5° by 5° and are divided into three altitude ranges. The vertical bins approximately correspond to the Marine Boundary Layer (MBL)/lower troposphere (0-2 km), the midtroposphere (2-8 km), and the upper troposphere (8-12 km). Plates 5-7 show the corresponding 5° by 5° patch plots for ACE 1. The ACE-1 data are described by Blake *et al.* [1999], and are displayed here in the same form as PEM-Tropics A in order to facilitate comparison between the two data sets.

4.1 Southwestern Pacific

Plates 2-7 reveal that high average mixing ratios of O_3 (45-80 ppbv) and trace gases characteristic of biomass burning emissions CO (75-115 ppbv), C_2H_6 (390-750 pptv), C_2H_2 (65-215 pptv), and CH_3Cl (560-600 pptv) were observed in the midtroposphere (2-8 km) over the southwestern Pacific during both PEM-Tropics A and ACE 1. For PEM-Tropics A, this enhanced region extended from the southern tip of New Zealand to about $10^\circ S$ and east to about $155^\circ W$. Ozone mixing ratios of as much as 80 parts per billion by volume (ppbv) were encountered on a majority of flights versus a typical background of 10-40 ppbv [Bodhaine *et al.*, 1993]. The $5^\circ \times 5^\circ$ average mixing ratios shown in Plates 2-7 conceal the fact that on several days, O_3 mixing ratios exceeded 100 ppbv, with the most spectacular enhancement reaching 140 ppbv on a flight north out of Fiji on October 1, 1996. By contrast, C_2Cl_4 mixing ratios remained at background levels at all altitudes over the southwestern Pacific during PEM-Tropics A and ACE 1 (approximately 1.4 pptv and 1.5 pptv, respectively) (Plates 4 and 7). These results indicate that a large portion of the southwestern Pacific was experiencing heavy burdens of biomass burning emissions (CO , C_2H_6 , and C_2H_2 , and CH_3Cl) and secondary pollutants (O_3), but no significant urban influence (low C_2Cl_4).

The southwestern Pacific enhancements observed during PEM-Tropics A originated from the west and were in the form of distinct layers of pollution [Fuelberg *et al.*, 1999; Fenn *et al.*, this issue]. Such layers were encountered during all but one flight over the remote South Pacific (west of $100^\circ W$).

However, in the southwestern region (west of about $155^\circ W$ and between 10° and $55^\circ S$) they typically were more coherent and contained higher mixing ratios of CO , O_3 , C_2H_6 , C_2H_2 , and CH_3Cl .

Figure 1 shows a vertical profile through one layer observed between about 3 and 7 km altitude. The profile was sampled by the DC-8 near Tahiti on September 5, 1996. The layer exhibited elevated mixing ratios of CO , O_3 , C_2H_6 , C_2H_2 , and CH_3Cl , but C_2Cl_4 remained at background levels. Enhanced mixing ratios of photochemical species other than O_3 , including PAN, alkyl nitrates, nitric acid, formic acid and acetic acid, were also observed in such layers [Schultz *et al.*, 1999; Talbot *et al.*, 1999].

The layer shown in Figure 1 was observed by the airborne differential absorption lidar (DIAL) system for more than 400 km in a north-south direction [Fenn *et al.*, this issue] and was far removed from any major landmasses or sources, implying a quite remarkable degree of air mass coherence. No direct measurements of the east-west extension of this pollution plume could be made. However, because the winds at the plume altitude were predominantly from the west (see below), the east-west plume dimensions were probably much larger than those observed along the longitudinal coordinate.

Incomplete combustion of biomass material is the only common source for the combination of elevated CO , C_2H_2 , C_2H_6 , and CH_3Cl in Figure 1. The lack of enhancement of C_2Cl_4 in the plume indicates that urban pollutants did not contribute substantially to the chemical composition of this layer.

Two sets of complementary observations are useful in identifying the time and place of origin of these pollution events. Backward trajectories can identify the probable path of the plume, and changes in the chemical composition with time can constrain the time of formation [Mauzerall *et al.*, 1998]. Plate 8 displays trajectories calculated for 10 days backward from $15^\circ S$, $155^\circ W$ for three altitudes of the descent [Fuelberg *et al.*, 1996, 1999] illustrated in Figure 1. All trajectories arriving at the altitude of the biomass burning layer (600 hPa, ~ 4.2 km, shown in red in Plate 8) originated from the west and covered long distances during the 10 day period. These air masses were near the east coast of Australia approximately 5 days earlier and were over southern Africa 9-10 days prior to reaching the flight track. The trajectories had descended approximately 5 km during the 10 day period, consistent with very dry air observed in the plumes. In situ temperature profiles along the 4.2 km portion of the flight track exhibit prominent temperature inversions with bases near 3.2 and 6.7 km. These inversions have the classic appearance of subsidence; that is, humidity decreases with altitude as temperature increases. The baseline altitudes correspond to the top and bottom of the polluted layer. Because inversions are stable layers that suppress vertical mixing, these subsidence-induced inversions may be important factors in explaining the high degree of layer coherence that was observed well away from the pollution source. Similar subsidence inversions were observed on many other flights [Fuelberg *et al.*, 1999].

Most trajectories arriving below the pollutant plume at 850 hPa (~ 1.5 km, green in Plate 8) originated from the west, with a few that passed near the coast of Australia 8-10 days prior to their arrival along the flight track. This aged marine air would be expected to contain relatively low (10-40 ppbv) O_3 concentrations [Bodhaine *et al.*, 1996], consistent with the

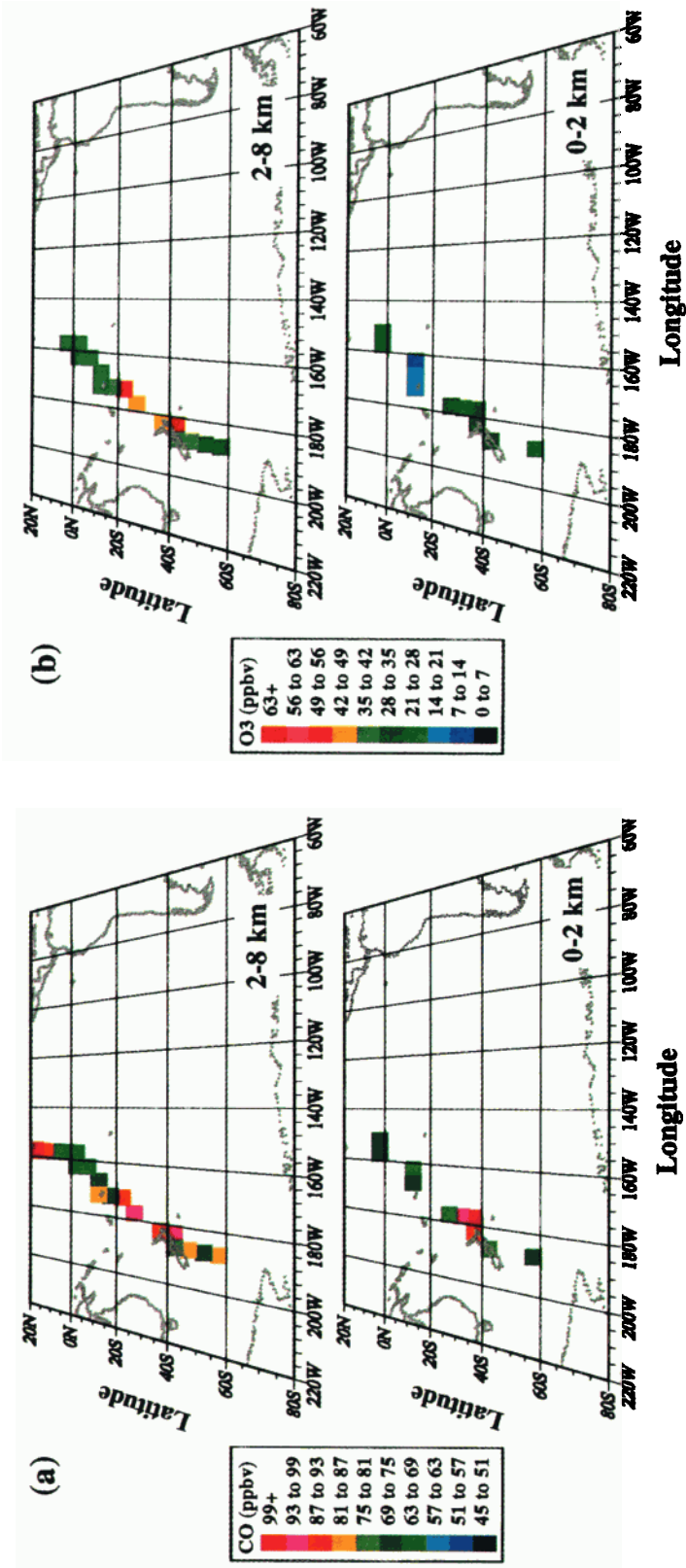


Plate 5. Spatial distribution of (a) CO and (b) O₃ over the Pacific Ocean during ACE-1 for two altitude ranges (0-2 and 2-8 km).

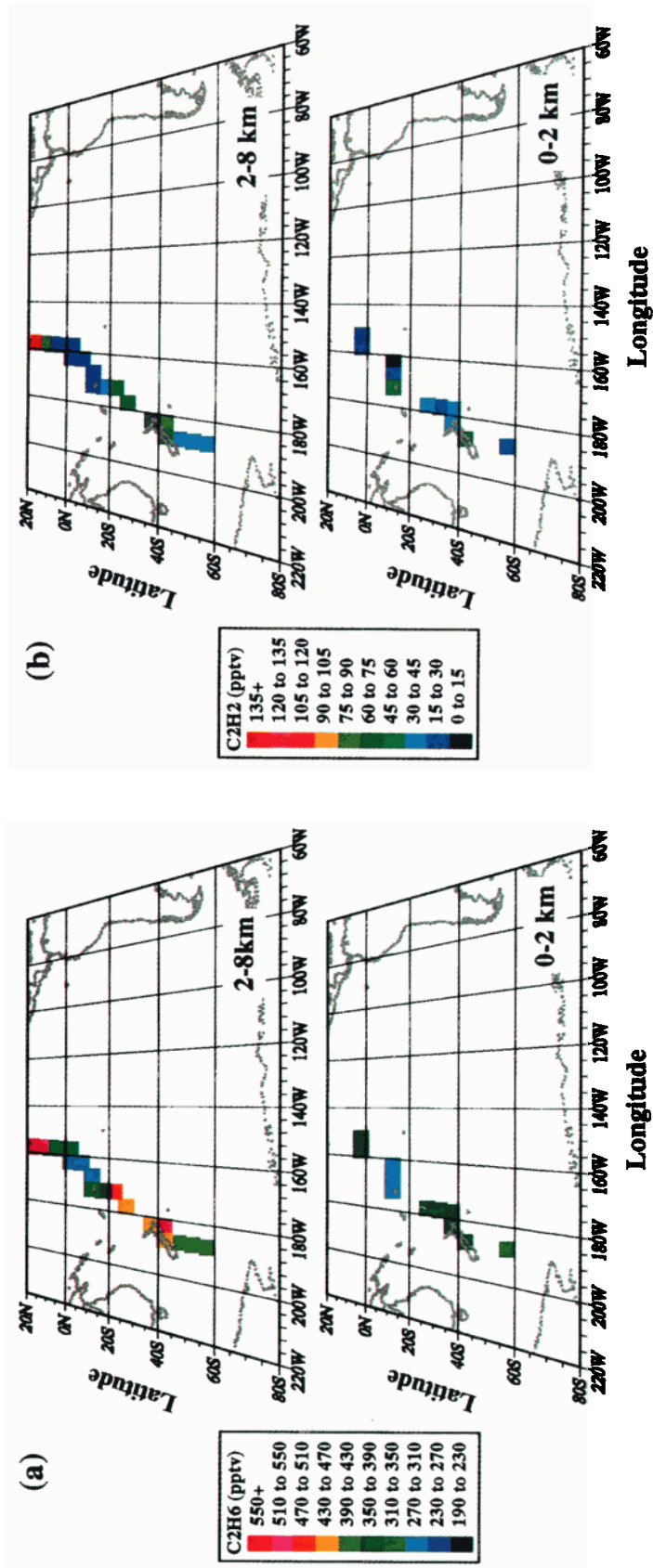


Plate 6. Same as for Plate 5 but for (a) C_2H_6 and (b) C_2H_2 .

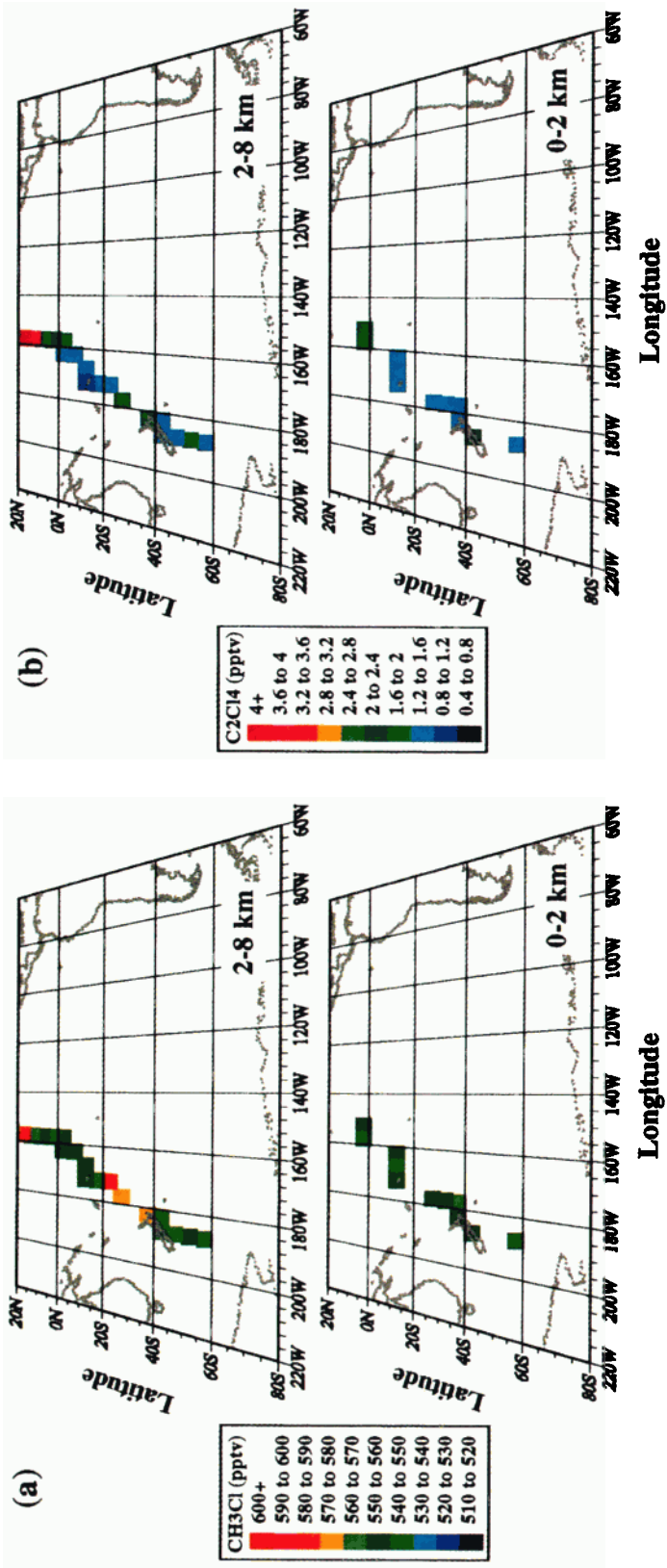


Plate 7. Same as for Plate 5 but for (a) CH_3Cl and (b) C_2Cl_4 .

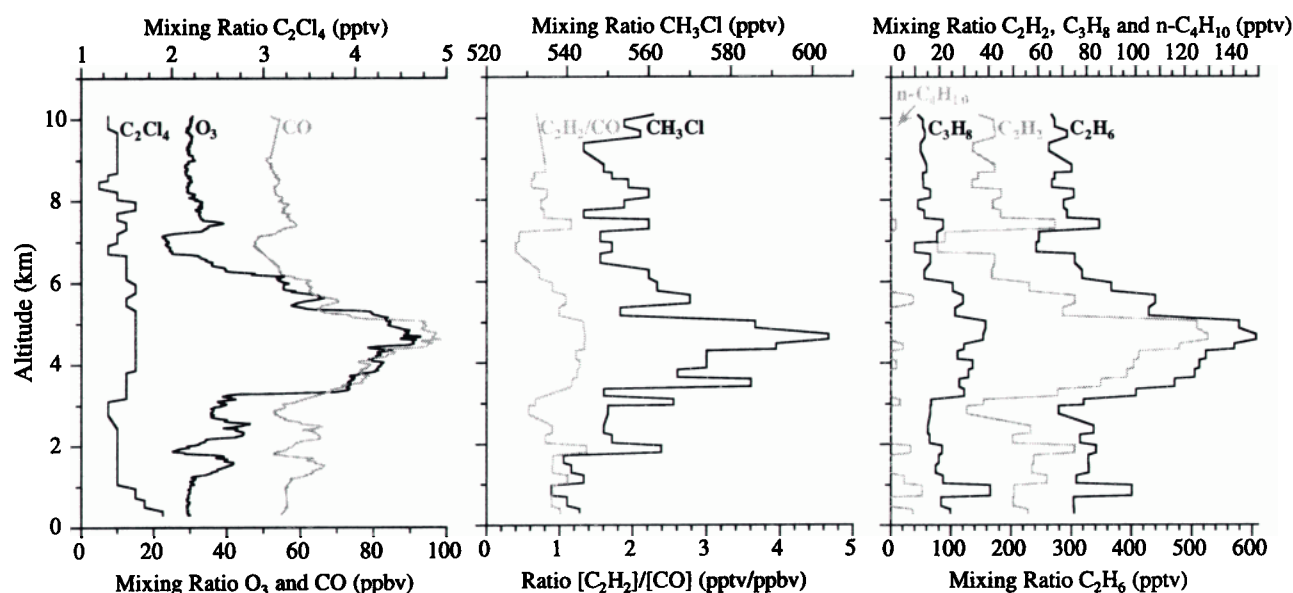


Figure 1. Vertical profiles of C_2Cl_4 , O_3 , CO , $\text{C}_2\text{H}_2/\text{CO}$, CH_3Cl , $n\text{-C}_4\text{H}_{10}$, C_2H_2 , and C_2H_6 through a layer of continental pollution that was sampled by the DC-8 near Tahiti during PEM-Tropics A on September 5, 1996.

observations at 1.5 km (Figure 1). Trajectories intercepting the flight path at a much higher altitude (300 hPa, ~ 9.2 km, blue in Plate 8) mostly remained over the ocean while skirting portions of Indonesia. The mixing ratios of O_3 , CO , C_2H_6 , C_2H_2 and C_2Cl_4 associated with trajectories arriving at both 300 and 850 hPa (Plate 8) are all consistent with their similar tropical maritime histories.

Although C_3H_8 and $n\text{-butane}$ ($n\text{-C}_4\text{H}_{10}$) are emitted during biomass burning [Blake *et al.*, 1996b], these relatively short-lived gases were at or near background mixing ratios in the plume layer (Figure 1). Tropical midtropospheric lifetimes are approximately 10 days for C_3H_8 and 4 days for $n\text{-C}_4\text{H}_{10}$. In addition, ratios of $\text{C}_2\text{H}_2/\text{CO}$ were low (≈ 1.0 pptv/ppbv) in the plume (Figure 1), consistent with biomass burning emissions that have been aged >5 days [e.g., Gregory *et al.*, 1998; Sandholm *et al.*, 1992; Smyth *et al.*, 1996]. We therefore

suggest that relatively fresh Australian biomass burning emissions were unlikely to have significantly influenced the observed layer.

Many trajectories calculated for the different biomass burning layers observed over the southwestern Pacific during PEM-Tropics A reached as far west as South America in 10 days or less via upper tropospheric high winds [Fuelberg *et al.*, 1999; Board *et al.*, this issue]. The biomass-burning-enhanced air masses in the midtroposphere over the South Pacific during ACE 1 also originated from the west [Blake *et al.*, 1999]. These ACE 1 air masses most likely had advected from fires in southern Africa or South America, but an Australian source could not be ruled out completely [Blake *et al.*, 1999]. Board *et al.* [this issue] used back trajectory calculations to show that during PEM-Tropics A, air masses exhibiting a weak biomass burning signature arrived in low-

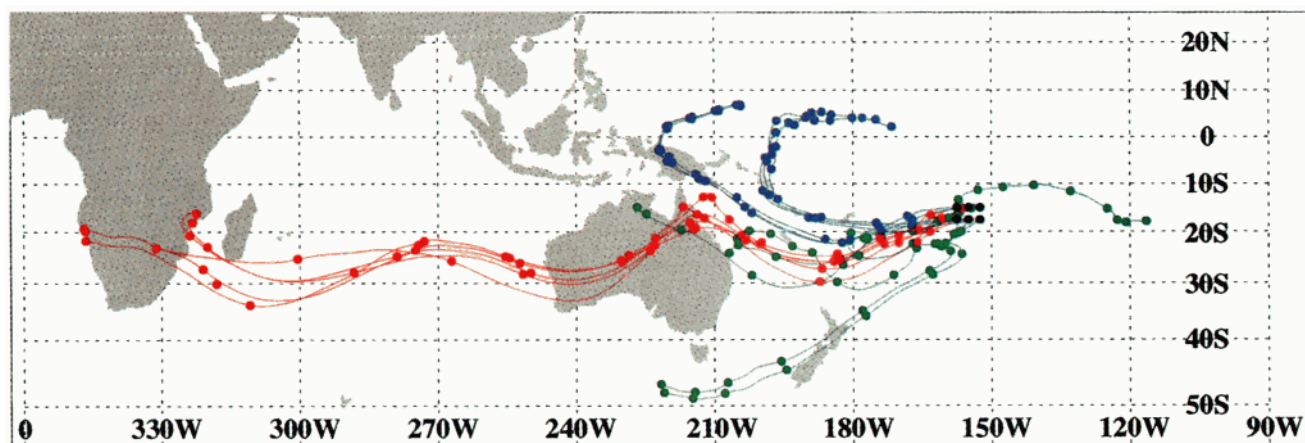


Plate 8. Ten day backward trajectories (4) arriving at 850 hPa (~ 1.5 km, green), 600 hPa (~ 4.2 km, red), and 300 hPa (~ 9.2 km, blue) near 15°S , 155°W at 0000 UTC, September 6, 1996. The colored circles on each trajectory denote locations at daily intervals.

latitude parts of the western and central South Pacific from Australia and southeastern Asia by way of Australia. However, these air parcels traveled shorter distances, and many were observed at lower altitudes than those that originated from South America or Africa.

Using data collected in encounters with South American and southern African biomass burning plumes during the NASA TRACE-A project in autumn 1992, Mauzerall *et al.* [1998] reported $\Delta C_2H_6/\Delta CO$, $\Delta C_2H_2/\Delta CO$, and $\Delta C_3H_8/\Delta CO$ values for 11 fresh plumes (typically less than half a day old) of 7.5, 4.2, and 2.4 pptv/ppbv respectively, and 8.0, 2.8, and 1.2 pptv/ppbv respectively for 14–16 old or aged plumes (about 1 week old). (The symbol Δ represents the molar excess for each trace gas with respect to background concentrations.) Because their atmospheric lifetimes decrease in the order C_2H_6 , CO , C_2H_2 , and C_3H_8 , the aging of a plume should be accompanied by a decrease in the $\Delta C_2H_2/\Delta CO$ and $\Delta C_3H_8/\Delta CO$ ratios and a slow increase in the $\Delta C_2H_6/\Delta CO$ ratio. For all data collected in midtroposphere (4–8 km) over the South Pacific PEM-Tropics A, respective enhancement ratios for $\Delta C_2H_6/\Delta CO$, $\Delta C_2H_2/\Delta CO$, and $\Delta C_3H_8/\Delta CO$ of 8.3, 2.4 and 0.9 (Figure 2) are consistent with a lifetime somewhat longer than 1 week. These results are also consistent with the analysis of Dibb *et al.* [this issue] who employed growth of the natural radionuclide tracer lead-210 (^{210}Pb), combined with the mixing ratios of 4 NMHCS plus CO to help constrain the ages of the intercepted plumes. They calculate that a significant fraction of plumes were in the 5–14 day old range.

Positive correlations were observed for the biomass burning tracer CH_3Cl versus CO over the southwestern Pacific midtroposphere during PEM-Tropics A (Figure 3). The midtropospheric CH_3Cl enhancements during ACE 1 (Plate 7) also indicated that the southwestern Pacific region had been influenced by biomass burning. The correlation of CH_3Cl with CO in these air masses was not significant, but a positive correlation was observed for CH_3Cl versus C_2H_6 over the South Pacific in the 4–8 km altitude range during ACE 1 (Figure 3).

The lack of correlation between C_2Cl_4 and the combustion tracers CO and C_2H_6 in Figures 2 and 4 confirms the absence of urban influence, indicating biomass burning as the source of the large-scale pollution observed in the southwestern Pacific region during PEM-Tropics A and the plumes encountered during ACE 1.

Previous studies have observed deep convection of biomass burning emissions from Brazilian fires [Pickering *et al.*, 1996] and the eastward transport of air from the east coast of Africa into the Indian Ocean [Thompson *et al.*, 1996]. Similarly, during the PEM-Tropics A experiment, deep convection likely carried combustion by-products into the upper troposphere, where they were transported rapidly eastward into the South Pacific region [Fuelberg *et al.*, 1999]. A similar transport mechanism could also account for the ACE-1 plume observations. Matsueda *et al.* [1998] report a strong seasonal cycle in the upper troposphere, with a maximum in CO at mid latitudes of the Southern Hemisphere during

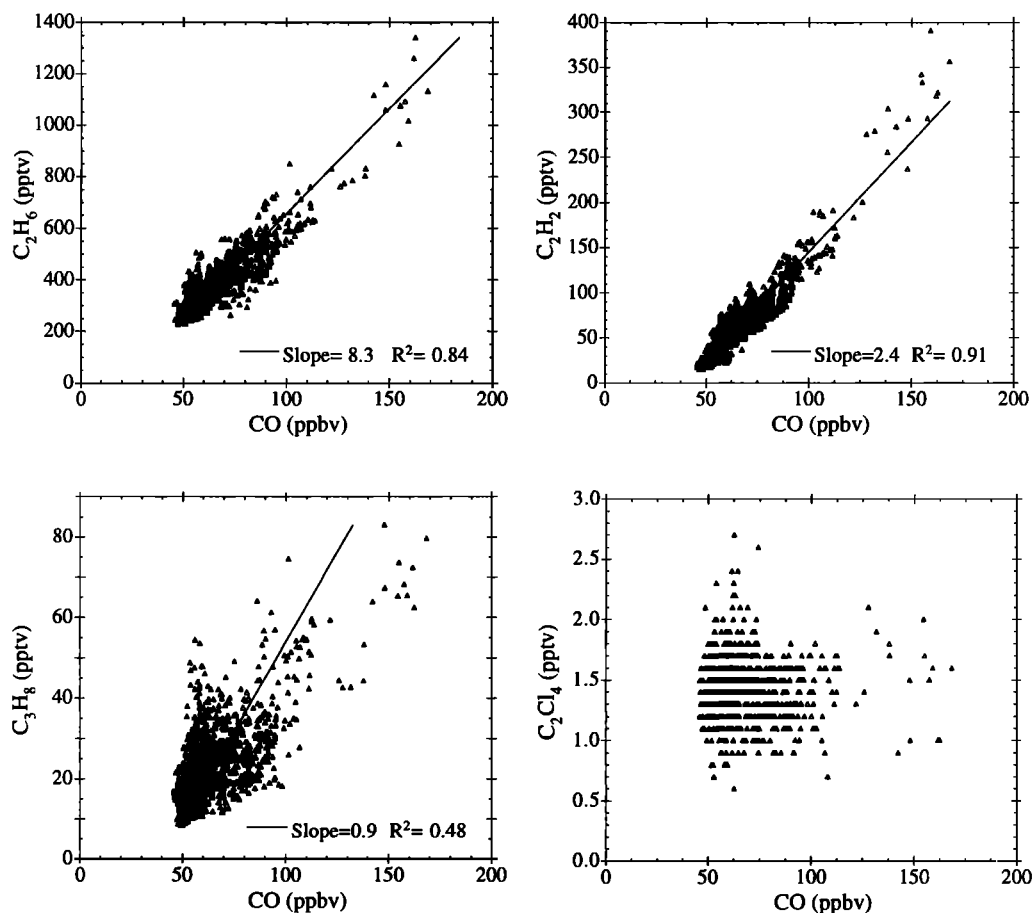


Figure 2. Correlation plots of C_2H_6 versus CO , C_2H_2 versus CO , C_3H_8 versus CO , and C_2Cl_4 versus C_2H_6 for all PEM-Tropics A data collected in the Southern Hemisphere between 4 and 8 km south and east of Fiji and west of $100^\circ W$ (i.e., all the data collected during flights out of Tahiti, Easter Island, and New Zealand).

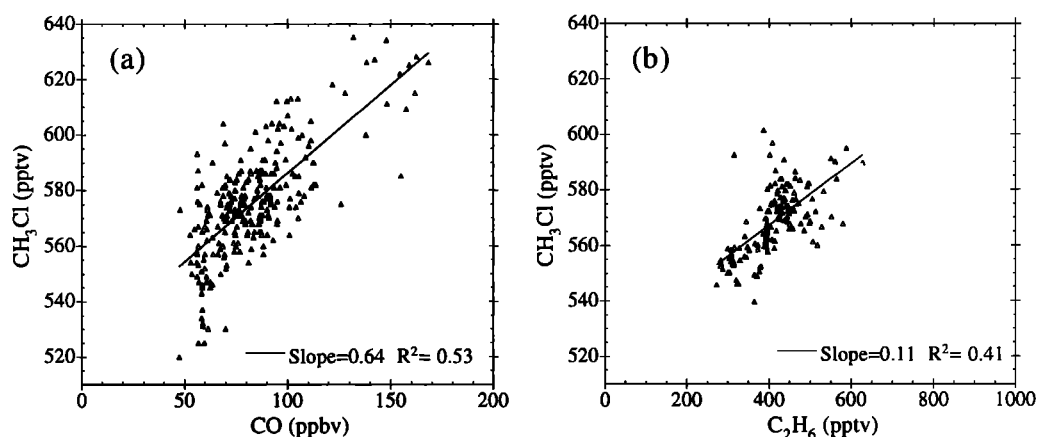


Figure 3. (a) Same as for Figure 2 but for CH_3Cl versus CO . (b) Correlation plots of CH_3Cl versus C_2H_6 for all ACE-1 data collected at altitudes > 4 km and 0° – 55°S during the southbound latitudinal transect.

October–November of both 1994 and 1995 (the two years in which measurements were made during this season). They suggest that long-range transport of combustion materials via the upper troposphere is much more frequent during the transitional period from the dry season to the wet season because of the onset of more active deep convection in the continental source regions.

Plates 2–4 show relatively low mixing ratios of CO , O_3 , C_2H_6 , C_2H_2 , and CH_3Cl , at low- and midaltitudes (0–8 km) in the tropical region to the northwest of Fiji, north of the South Pacific Convergence Zone (SPCZ). The low mixing ratios occurred because the SPCZ provided a physical barrier to pollutants entering the South Pacific region from the west [Gregory *et al.*, 1999].

4.2 Easterly Outflow From South America

Elevated mixing ratios of gases characteristic of biomass burning emissions, including CO , CH_3Cl , C_2H_6 , C_2H_2 , and C_3H_8 , were observed in all altitude ranges during three local P-3B flights conducted from Guayaquil, Ecuador, September 18–23, 1996 (Plates 2–4). The mixing ratios of these gases were most elevated over background values in the altitude range 1.5–4 km (Figure 5). The high values for $\text{C}_2\text{H}_2/\text{CO}$ (Figure 5) indicate that many of the sampled air masses were relatively fresh, compared to the plumes arriving from the west discussed

earlier. Mixing ratios of the urban tracer C_2Cl_4 were usually close to background levels of about 1.4 pptv during these Guayaquil local flights (Plate 4 and Figure 5). However, four samples collected at low altitude during Guayaquil landings exhibited C_2Cl_4 mixing ratios between 4 and 9 pptv and showed very high C_3H_8 mixing ratios (between 500 and 1000 pptv), indicating urban emissions.

Regressions for C_2H_6 , C_2H_2 , and CH_3Cl versus CO in the altitude range 1.5–4 km for the three Guayaquil local flights were highly correlated (Figure 6). The corresponding enhancement ratios for C_2H_6 , C_2H_2 , and CH_3Cl versus CO (7.4, 2.9, and 0.73 pptv/ppbv, respectively) were remarkably similar to those observed in biomass burning plumes during TRACE A [Blake *et al.*, 1996b; Mauzerall *et al.*, 1998]. The good correlations for C_2H_6 , C_2H_2 , and CH_3Cl versus CO , and generally poor correlations for C_2Cl_4 versus CO , suggest that the air masses sampled just off the coast of South America were most strongly influenced by biomass burning emissions, rather than by urban emissions.

Numerous backward trajectories for different locations along the Guayaquil local flight tracks traveled over South America [Fuelberg *et al.*, 1999], including regions of Brazil where biomass burning usually is widespread during September [Fishman *et al.*, 1996; Olson *et al.*, 1999]. Figure 7 shows 10 day backward trajectories for air masses arriving at 700 hPa (~ 3 km) along the P-3B mission 17 track. These trajectories, combined with the air mass chemical characteristics described above, indicate that biomass burning emissions were transported off the west coast of South America into the South Pacific basin [Fuelberg *et al.*, 1999]. (Note that trajectories were terminated if they intersected the Andes.)

Polluted continental outflow was also encountered between 8.0 and 9.5 km at the northernmost extent (7°S) of a flight north from Easter Island on September 10, 1996. This air mass exhibited C_3H_8 mixing ratios of nearly 300 pptv compared to background levels of approximately 20 pptv. Ethane mixing ratios were about 900 pptv above background levels. However, relatively small increases in the combustion tracers C_2H_2 and CO were observed (about 50 pptv and 25 ppbv above background, respectively). Methyl chloride and C_2Cl_4 remained at background levels. Enhancement ratios for C_3H_8 versus CO and C_2H_6 versus CO were much higher than those observed for the biomass burning plumes near Guayaquil (about 11 and 36 pptv/ppbv for $\Delta\text{C}_3\text{H}_8/\Delta\text{CO}$ and $\Delta\text{C}_2\text{H}_6/\Delta\text{CO}$,

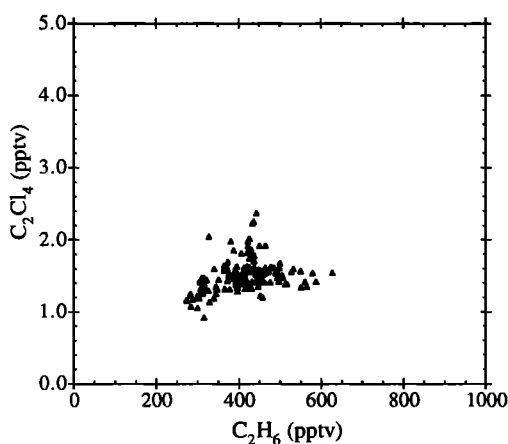
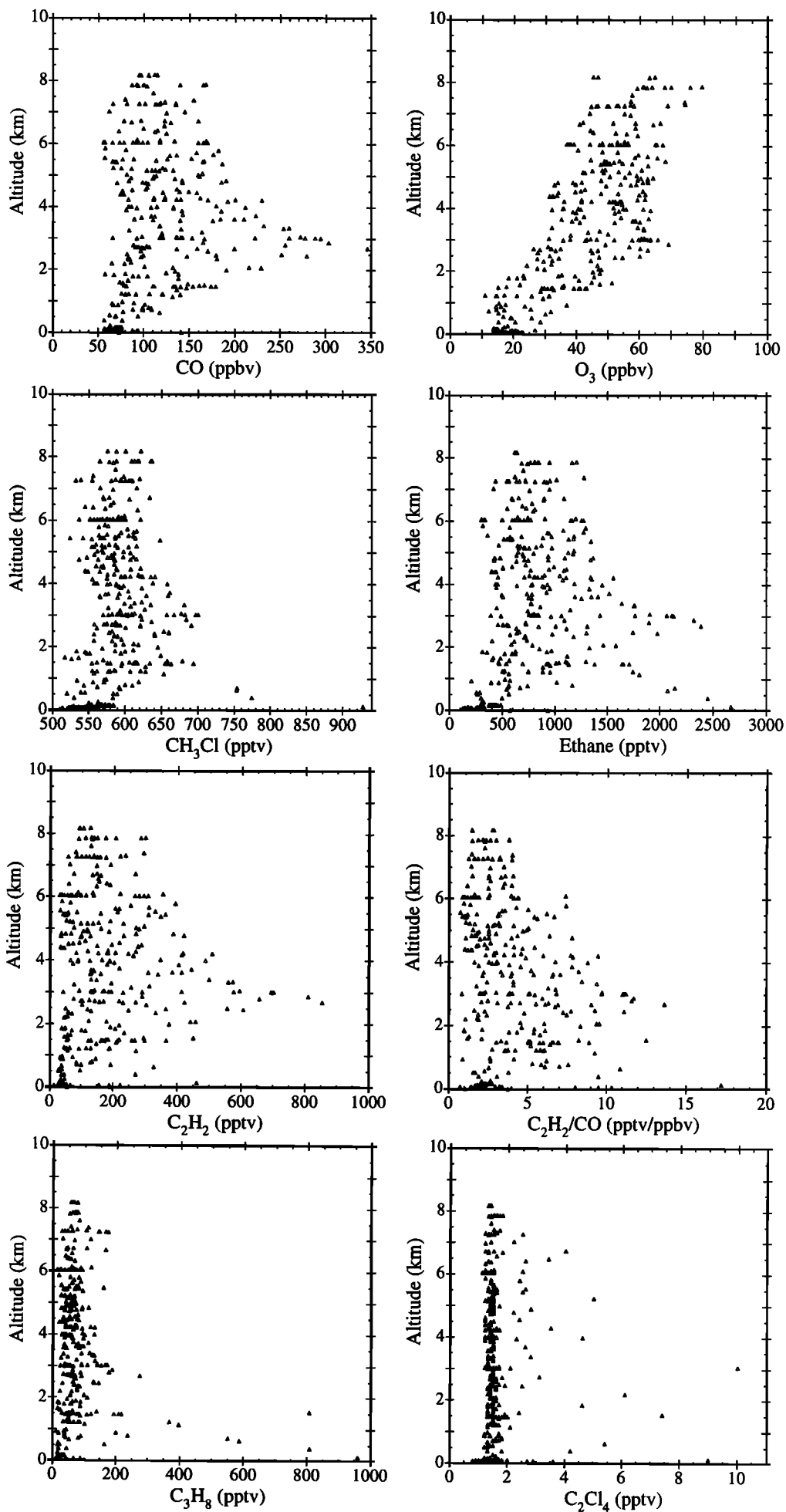


Figure 4. Same as for Figure 3b but for C_2Cl_4 versus C_2H_6 .



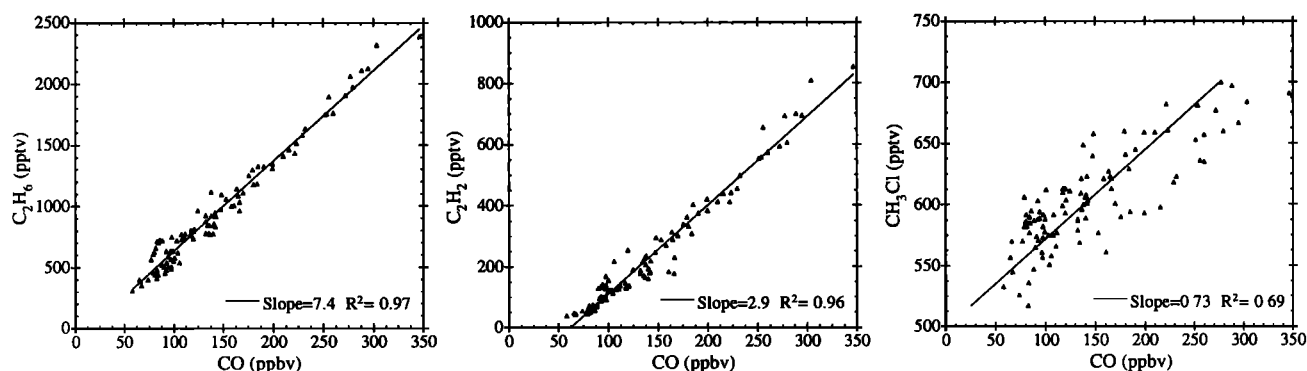


Figure 6. Correlation plots of C_2H_6 versus CO, C_2H_2 versus CO, and CH_3Cl versus CO for the altitude range 1.5–4 km for three local P-3B flights (17–19) conducted from Guayaquil, Ecuador, September 18–23, 1996, as part of PEM-Tropics A.

respectively, compared to 0.55 and 7.4 pptv/ppbv, respectively for the Guayaquil plumes). The ratio for CH_4 versus CO was approximately 20 times that typical of biomass burning emissions [Blake *et al.*, 1996b]. Ten-day back trajectories for the plume (Figure 8) originate from the northeast of the flight track near Central America and northern South America [Fuelberg *et al.*, 1999]. The trajectories indicate that emissions from oil drilling and/or natural gas fields located in Venezuela are a possible source of the gases observed in this air mass. Urban natural gas and/or LPG leakage may also have contributed to the observed enhancements [Blake and Rowland, 1995].

5. Impact of Biomass Burning on the Chemistry of the Remote South Pacific

We have shown that the enhancements in numerous trace gases over the south central Pacific are the result of aged biomass burning. The positive correlations between O_3 and CO, C_2H_6 and C_2H_2 shown in Figure 9 establish a direct link between elevated levels of O_3 and biomass burning emissions over the South Pacific in midtroposphere (4–8 km) west of $100^\circ W$. Figure 9 also reveals good positive correlations between O_3 and CO, C_2H_6 and C_2H_2 for all ACE-1 data collected in the South Pacific midtroposphere during the southbound latitudinal transect (Plate 1).

The O_3 versus CO regression slopes of 1.5 and 1.9 ppbv/ppbv for PEM-Tropics A and ACE 1, respectively, are in reasonable agreement (Figure 9). However, they are greater than the average O_3 /CO enhancement ratio of 0.74 ppbv/ppbv calculated by Mauzerall *et al.* [1998] for approximately one week old biomass burning plumes observed in the South Atlantic region during TRACE A. We recall that many of the South Pacific plumes were aged more than one week so may have been influenced by the photochemical loss of CO, which causes the O_3 /CO ratio to increase with age [Mauzerall *et al.*, 1998]. Net photochemical production of O_3 was calculated to continue at altitudes above about 6 km as the plumes were advected over the South Pacific during PEM-Tropics A [Schultz *et al.*, 1999]. This source may also have contributed to the high Pacific O_3 /CO ratios.

The above results show that the chemistry of the midtroposphere over the South Pacific was profoundly affected by the products of Southern Hemispheric biomass burning during both 1995 and 1996. The observations during both PEM-Tropics A and ACE 1 (Plates 2–7) further suggest that the effects of biomass burning were not confined to the late August–early October time period covered by PEM-Tropics A. Instead, they appear to extend at least into the early November ACE-1 period, at least during 1995. Southern African biomass burning activity typically peaks between July and September [Justice *et al.*, 1996], but NOAA-11 satellite AVHRR images reveal that both southern African and South American fires continued into November for both 1992 and 1993. Satellite data for November 1995 are not currently available, although fires associated with the African savanna ecosystem appear to have a similar geographic range and distribution from year to year [Cahoon *et al.*, 1992]. Matsueda *et al.* [1998] report a maximum in CO at midlatitudes of the Southern Hemisphere during October–November 1994 and 1995.

Northbound ACE-1 flights conducted in mid-December 1995 following a more westerly route (from Hobart to Brisbane, Australia, and continuing to Fiji and Christmas Island) revealed no evidence of biomass burning influence in the mid-troposphere.

6. Biomass Burning Impact on the Vertical Structure of the Troposphere

Figure 10 shows the vertical distribution of trace gases for background and relatively perturbed conditions over the South Pacific during PEM-Tropics A. For this figure, all Southern Hemisphere data collected in the southwestern and central South Pacific (south and east of Fiji to $100^\circ W$) have been segregated into bins defined by CO mixing ratios <55 ppbv and CO >70 ppbv. The average and median CO values for the entire data set were 70 and 71 ppbv, respectively. A histogram distribution showed the CO mixing ratios to be skewed to give a peak mixing ratio of 57 ppbv and cluster of samples with CO greater than about 65 ppbv, representing the numerous biomass burning layers described earlier. Samples with CO mixing ratios >70 ppbv were chosen to represent air

Figure 5. Vertical distribution of CO, O_3 , CH_3Cl , C_2H_6 , C_2H_2 , C_2H_2/CO , C_3H_8 , and C_2Cl_4 for three local P-3B flights (17–19) conducted from Guayaquil, Ecuador, September 18–23, 1996, as part of PEM-Tropics A.

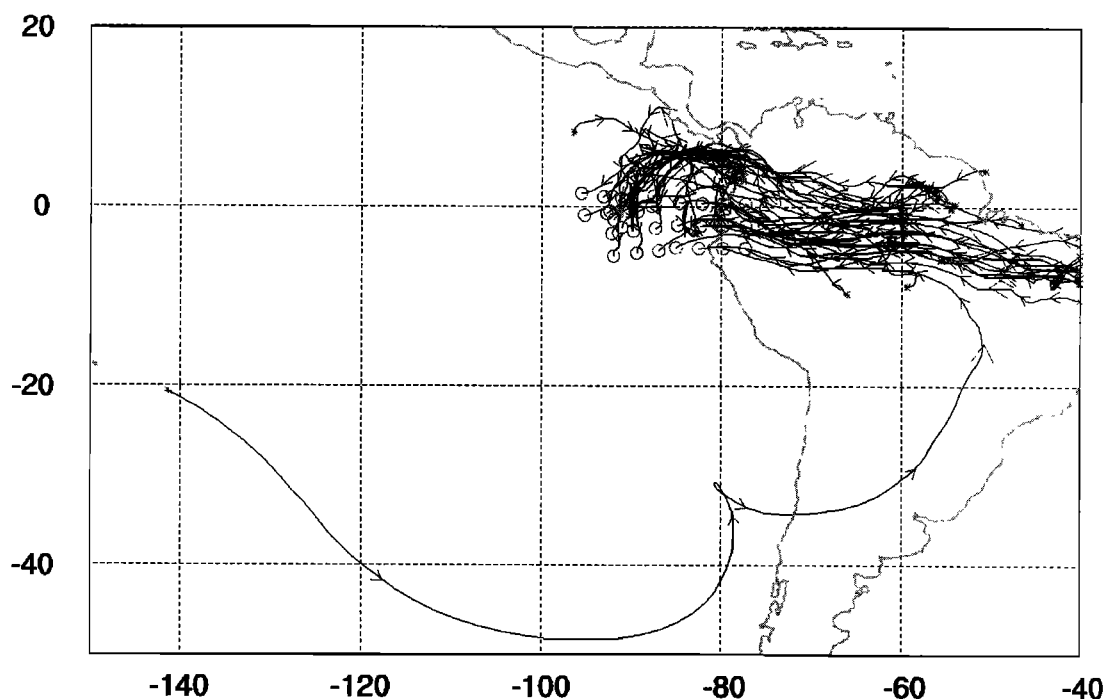


Figure 7. Ten day backward trajectories arriving at 700 hPa along the PEM-Tropics A P-3B flight 17 track at 0000 UTC September 17, 1996. Small arrows denote locations at daily intervals; large arrows denote locations at 5 day intervals.

masses that had been influenced by pollution. The subset of data with $\text{CO} < 55$ ppbv reflected air masses that were near "background" levels, i.e., were relatively free of the impact from recent biomass burning sources. The samples were also divided into 2 km altitude bins. The average number of

samples per bin was 90, with a range between 28 and 173 samples/bin.

Average mixing ratios of CO , C_2H_6 , and C_2H_2 were greater than the subset of data with $\text{CO} > 70$ ppbv compared to $\text{CO} < 55$ ppbv throughout the altitude range shown in Figure 10. Comparable results were obtained for a cutoff of $\text{CO} > 75$ ppbv. The most significant enhancements over background (i.e., no overlap of their respective $\pm 1\sigma$ variations) were observed in the 2–8 km altitude range for CO (35 ppbv), C_2H_6 (217 pptv), and C_2H_2 (78 pptv). Each gas exhibited almost no trend in average unperturbed ($\text{CO} < 55$ ppbv) mixing ratio with altitude (Figure 10).

By contrast, C_3H_8 in perturbed air masses showed relatively small and insignificant ($\pm 1\sigma$) increases above background in the 2–8 km altitude range (Figure 10). The average lifetime of C_3H_8 in the tropical midtroposphere is approximately 10 days. Dilution as well as chemical loss, needs to be taken into account when considering aged plumes. However, the lack of significant midtropospheric (2–8 km) C_3H_8 perturbation supports plume transport times of the order of 2 weeks from biomass burning source regions. The urban tracer C_2Cl_4 exhibited no significant differences for $\text{CO} < 55$ ppbv and $\text{CO} > 70$ ppbv (Figure 10).

The long-lived (approximately 1 year) biomass burning gases CH_3Cl and CH_3Br [Blake *et al.*, 1996b] displayed somewhat elevated midtropospheric (2–8 km) mixing ratios for $\text{CO} > 70$ ppbv (Figure 10), with increases of approximately 23 and 0.35 pptv, respectively. The ratios of these CH_3Cl and

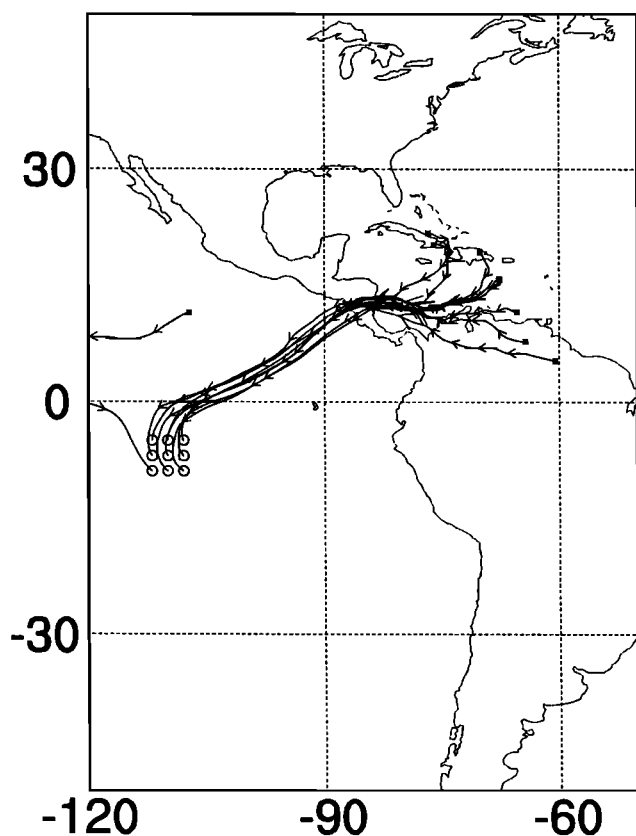


Figure 8. Ten day backward trajectories arriving at 250 hPa along the northerly part of the PEM-Tropics A DC-8 flight 8 track at 1200 UTC September 10, 1996. Small arrows denote locations at daily intervals; large arrows denote locations at 5 day intervals.

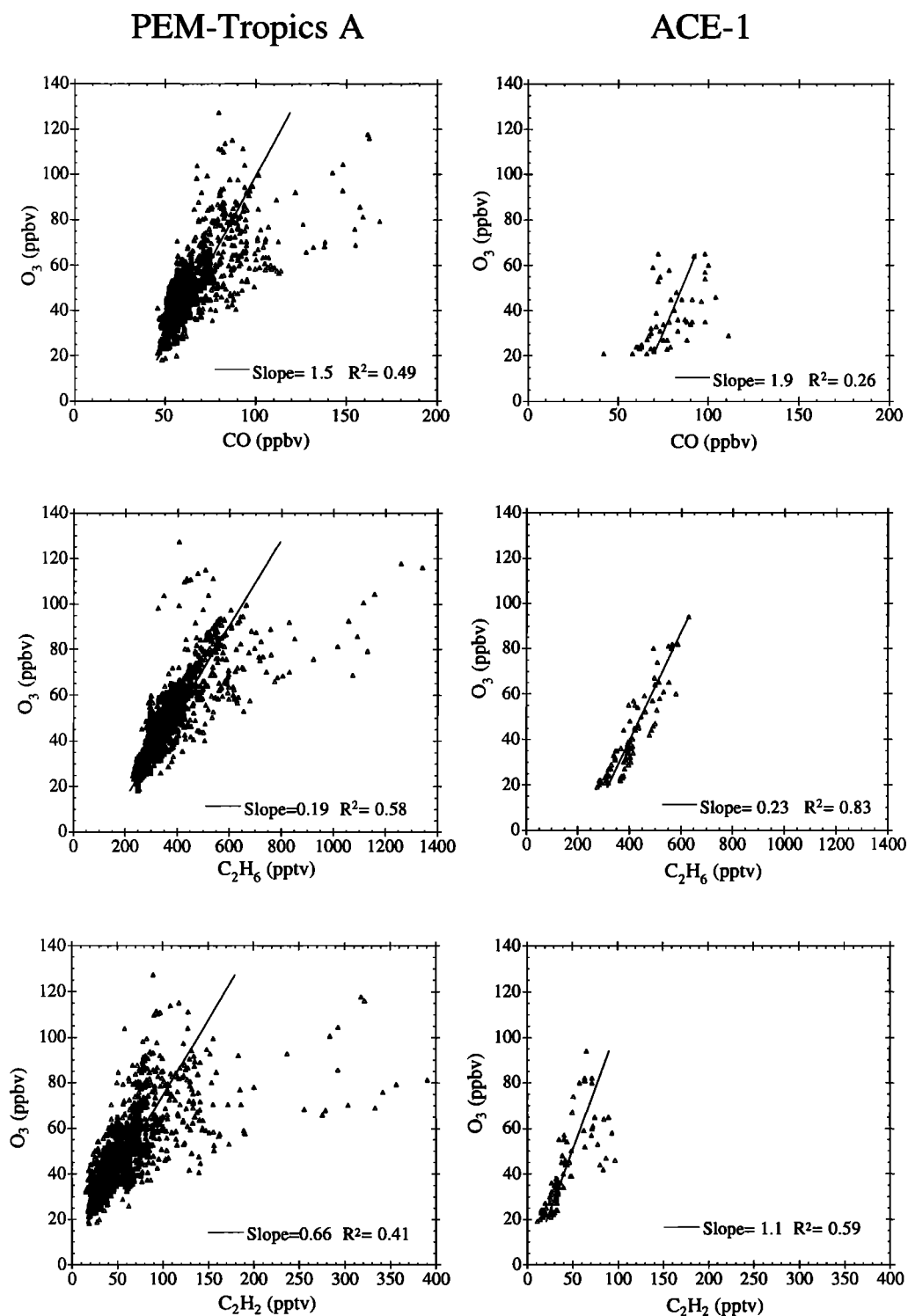


Figure 9. Correlation plots of O_3 versus CO, O_3 versus C_2H_6 , and O_3 versus C_2H_2 for all PEM-Tropics A data collected in the Southern Hemisphere between 4 and 8 km south and east of Fiji and west of $100^\circ W$ (i.e., all the data collected during flights out of Tahiti, Easter Island, and New Zealand) and for all ACE 1 data collected at altitudes > 4 km and 0° – $55^\circ S$ during the southbound latitudinal transect.

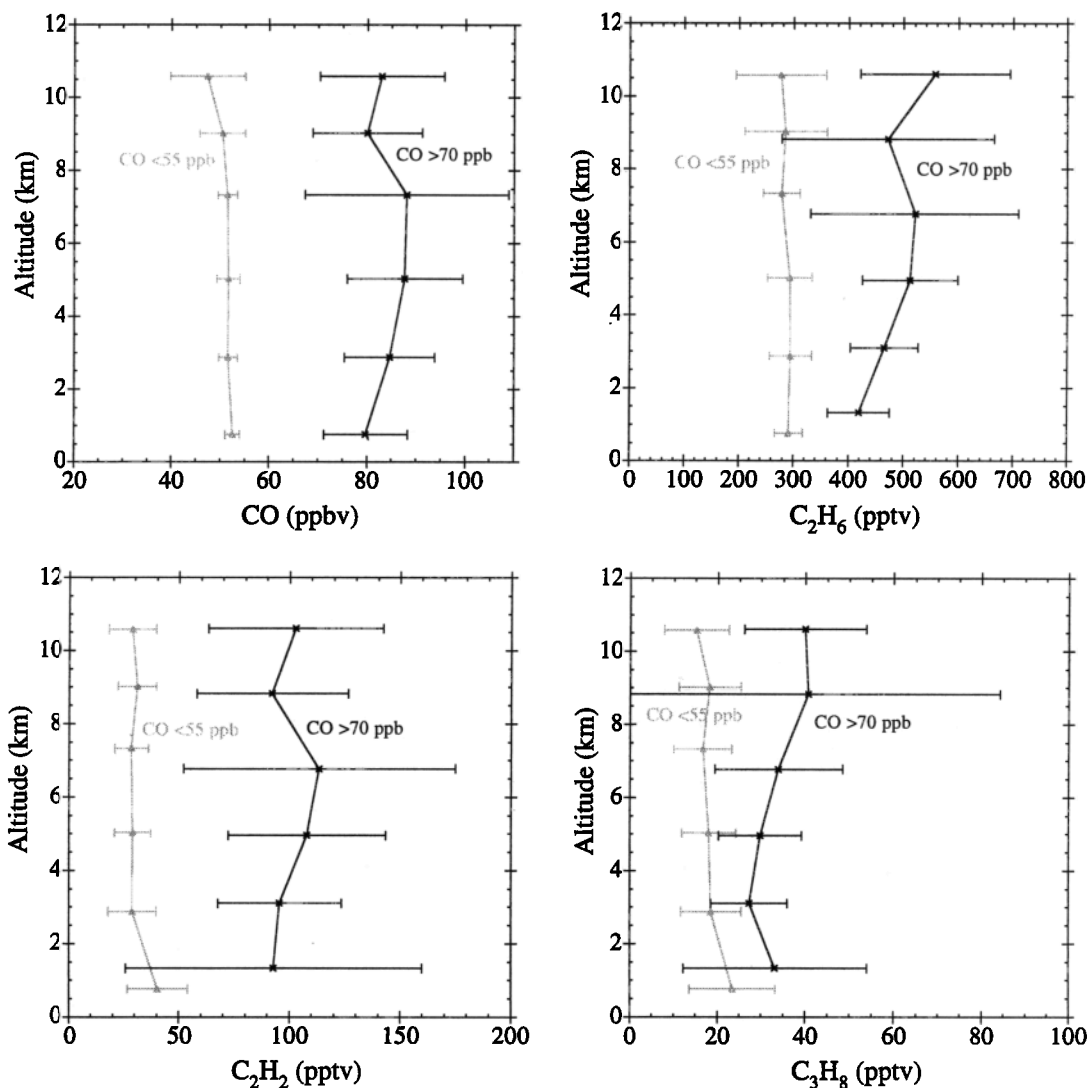


Figure 10. Vertical distribution of average mixing ratios for selected trace gases during the PEM-Tropics A experiment in the same geographical region as Figure 9. The data are grouped into bins having CO <55 ppbv and CO >70 ppbv representing relatively clean and perturbed conditions, respectively. Error bars are ± 1 standard deviation (σ).

CH₃Br enhancements relative to the corresponding CO increase of 35 ppbv are consistent with the $\Delta\text{CH}_3\text{Cl}/\Delta\text{CO}$ and $\Delta\text{CH}_3\text{Br}/\Delta\text{CO}$ ratios observed in the plumes from southern African and South American biomass fires [Andreae *et al.*, 1996; Blake *et al.*, 1996b]. The mixing ratios of CH₃Cl and CH₃Br in the clean MBL/lower troposphere below 2 km were similar, or slightly lower compared to the unperturbed free troposphere (Figure 10). This suggests that on average, the MBL was not significantly affected by net local oceanic emissions of these gases.

Average O₃ levels were significantly elevated ($\pm 1\sigma$) for CO >70 ppbv compared to CO <55 ppbv in the 2–8 km range (Figure 10). The average O₃ mixing ratios for the CO >70 ppbv mixing ratio bin for 2–8 km was 67 ppbv, compared to the background average of 33 ppbv. We recall that the observed midtropospheric CO mixing ratio enhancements over the South Pacific were caused by biomass burning. Therefore biomass burning sources caused O₃ levels to be

approximately double those for relatively clean background conditions during PEM-Tropics A. In fact, the CO <55 ppbv vertical profile for O₃ exhibits a "bulge" in the midtroposphere somewhat similar to that observed at high CO values (Figure 10). This suggests that even "background" O₃ may have been influenced by the widespread pollution encountered throughout the midtroposphere of the South Pacific region.

Results from a similar analysis employing the ACE-1 data gave a comparable 50–100% increase in O₃ mixing ratios for the biomass-burning-impacted plumes compared to background conditions for the 2–6 km altitude range. However, fewer data were available for these calculations.

7. Conclusion

This study has shown that coherent plumes containing nonurban combustion products from biomass fires in the tropical South Atlantic region and from South America were

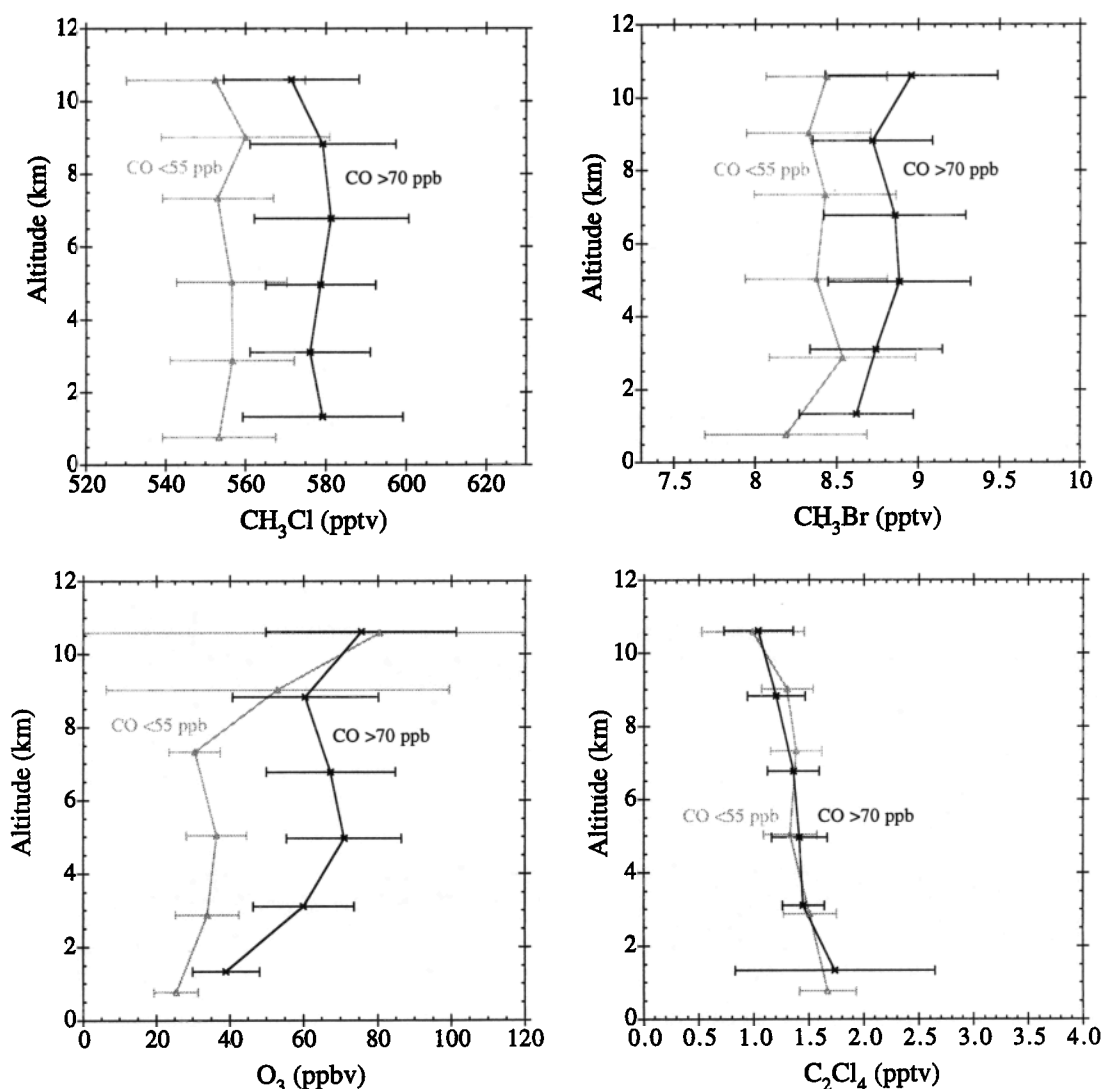


Figure 10. (continued)

observed over the remote South Pacific region. Biomass burning emissions also entered the South Pacific from an easterly direction over the coast of western South America. Photochemical production of O₃ from biomass burning emissions led to average midtropospheric O₃ mixing ratios approximately double those observed for relatively clean background conditions over the remote southwestern and central South Pacific. This O₃ enhancement has significant implications for the oxidizing power of the atmosphere and for greenhouse radiative forcing by O₃ on the upper troposphere. The influence of this biomass burning was observed during the November 1995 and August–October 1996 periods over even the most remote region of the tropical troposphere, a truly global perturbation of atmospheric chemistry.

Acknowledgments. We would like to express our appreciation to the excellent team at UCI who worked so hard in the laboratory, at the computer, and in the field to produce this NMHC and halocarbon data set, especially Doug Begbie, John Bilicska, Tai-Yih Chen, Nancy Conebeare, David Crosley, Kathy Farrow, Michael Gilligan, Adam Hill, Melissa Hills, Jenn Lapiere, Stacey Lasswell, Jan Latour, Brent Love, Geoff Luke, Murray McEachern, Russell Miller, and Christina Recoskie

and Nick Shrivane. We would like to acknowledge the ACE 1 CO measurement group, Greg Kok, Andre Prévôt, and Dick Schillawski. We are also grateful to Barbara Yu for her assistance during the projects. The PEM-Tropics A research was supported by the NASA Global Tropospheric Chemistry Experiment Program, grant NAG-1-1777. ACE 1 is a contribution to the International Global Atmospheric Chemistry (IGAC) core project of the International Geosphere-Biosphere Programme (IGBP) and is part of the IGAC Aerosol Characterization Experiments (ACEs).

References

- Andreae, M. O., Biomass burning: Its history, use, and distribution and its impact on environmental quality and global climate, in *Global Biomass Burning: Atmospheric, Climatic, and Biospheric Implications*, edited by J. S. Levine, MIT Press, Cambridge, Mass., 1991.
- Andreae, M. O., The influence of tropical biomass burning on climate and the atmospheric environment, in *Biogeochemistry of Global Change: Radiatively Active Trace Gases*, edited by R. S. Oremland, pp. 113–150, Chapman and Hall, New York, 1993.
- Andreae, M. O., E. Atlas, H. Cachier, W. R. Cofer III, G. W. Harris, G. Helas, R. Kopppmann, J. -P. Lacaux, and D. E. Ward, Trace gas and aerosol emissions from savanna fires, in *Biomass Burning and Global*

- Change, Vol. 1, edited by J. S. Levine, pp. 278-295, MIT Press, Cambridge, Mass., 1996.
- Andres, R. J., G. Marland, I. Fung, and E. Matthews, *Global Biogeochem. Cycles*, **10**, 419, 1996.
- Apel, E. C., J. G. Calvert, and F. C. Fehsenfeld, The Nonmethane Hydrocarbon Intercomparison Experiment (NOMHICE): Tasks 1 and 2, *J. Geophys. Res.*, **99**, 16,651-16,664, 1994.
- Bates, T. S., B. J. Huebert, J. L. Gras, F. B. Griffiths, and P. A. Durkee, The International Global Atmospheric Chemistry (IGAC) Project's First Aerosol Characterization Experiment (ACE 1): Overview, *J. Geophys. Res.*, **103**, 16,369-16,383, 1998.
- Blake, D. R., and F. S. Rowland, Urban leakage of liquefied petroleum gas and its impact on Mexico City air quality, *Science*, **269**, 953-956, 1995.
- Blake, D. R., D. F. Hurst, T. W. Smith Jr., W. J. Whipple, T.-Y. Chen, N. J. Blake, and F. S. Rowland, Summertime measurements of selected nonmethane hydrocarbons in the Arctic and subarctic during the 1988 Arctic Boundary Layer Expedition (ABLE 3A), *J. Geophys. Res.*, **97**, 16,559-16,588, 1992.
- Blake, D. R., T. W. Smith Jr., T.-Y. Chen, W. J. Whipple, and F. S. Rowland, Effects of biomass burning on summertime nonmethane hydrocarbon concentrations in the Canadian wetlands, *J. Geophys. Res.*, **99**, 1699-1719, 1994.
- Blake, D. R., T. Y. Chen, T. W. Smith Jr., C. J.-L. Wang, O. W. Wingenter, N. J. Blake, F. S. Rowland, and E. W. Mayer, Three-dimensional distribution of NMHCs and halocarbons over the northwestern Pacific during the 1991 Pacific Exploratory Mission (PEM-West A), *J. Geophys. Res.*, **101**, 1763-1778, 1996a.
- Blake, N. J., D. R. Blake, J. E. Collins Jr., G. W. Sachse, B. E. Anderson, J. A. Brass, P. J. Riggan, and F. S. Rowland, Biomass burning emissions of atmospheric methyl halide and hydrocarbon gases in the South Atlantic region, in *Biomass Burning and Global Change*, Vol. 2, *Biomass Burning in South America, Southeast Asia and Temperate and Boreal Ecosystems, and the Oil Fires of Kuwait*, edited by J. S. Levine, pp. 575-594, MIT Press, Cambridge, Mass., 1996b.
- Blake, N. J., D. R. Blake, T.-Y. Chen, J. E. Collins Jr., G. W. Sachse, B. E. Anderson, and F. S. Rowland, Distribution and seasonality of selected hydrocarbons and halocarbons over the western Pacific basin during PEM-West A and PEM-West B, *J. Geophys. Res.*, **102**, 28,315-28,331, 1997.
- Blake, N. J., et al., Aircraft measurements of the latitudinal, vertical, and seasonal variations of NMHCs, methyl nitrate, methyl halides, and DMS during ACE 1, *J. Geophys. Res.*, in press, 1999.
- Board, A. S., H. E. Fuelberg, G. L. Gregory, B. G. Heikes, M. G. Schultz, D. R. Blake, J. E. Dibb, S. T. Sandholm, and R. W. Talbot, Chemical characteristics of air from differing source regions during PEM-Tropics A, *J. Geophys. Res.*, this issue.
- Bodhaine, B., et al., *CMDL Summary Rep. 1992*, **21**, 30, 1993.
- Cahoon, D. R., B. J. Stocks, J. S. Levine, W. R. Cofer, and K. P. O'Neill, Seasonal distribution of African savanna fires, *Nature*, **359**, 812-815, 1992.
- Crutzen, P. J. and M. O. Andreae, Biomass burning in the tropics: Impact on atmospheric chemistry and biogeochemical cycles, *Science*, **250**, 1669-1678, 1990.
- Connors, V. S., P. C. Novelli, and H. G. Reichle Jr., Space shuttle views changing carbon monoxide in lower atmosphere, *Eos Trans., AGU*, **77**, (46) Fall Meet. Suppl., 466, 1996.
- Fenn, M. A., et al., Ozone and aerosol distributions and air mass characteristics over the South Pacific during the burning season, *J. Geophys. Res.*, this issue.
- Fishman, J., C. E. Watson, J. C. Larsen, and J. A. Logan, Distribution of tropospheric ozone determined from satellite data, *J. Geophys. Res.*, **95**, 3599-3617, 1990.
- Fishman, J., J. M. Hoell Jr., R. D. Bendura, R. J. McNeal, and V. W. J. H. Kirchhoff, NASA GTE TRACE A experiment (September-October 1992): Overview, *J. Geophys. Res.*, **101**, 23,865-23,879, 1996.
- Fuelberg, H. E., R. O. Loring Jr., M. V. Watson, M. C. Sinha, K. E. Pickering, A. M. Thompson, G. W. Sachse, D. R. Blake, and M. R. Schoeberl, TRACE-A trajectory intercomparison, 2, Isentropic and kinematic methods, *J. Geophys. Res.*, **101**, 23,927-23,939, 1996.
- Fuelberg, H. E., et al., A meteorological overview of the PEM-Tropics period, *J. Geophys. Res.*, **104**, 5585-5622, 1999.
- Gregory, G. L., et al., Chemical characteristics of Pacific tropospheric air in the region of the ITCZ and SPZ, *J. Geophys. Res.*, **104**, 5677-5696, 1999.
- Hao, W. M. and M.-H. Liu, Spatial and temporal distribution of tropical biomass burning, *Global Biogeochem. Cycles*, **8**, 495, 1994.
- Hoell, J. M., Jr., et al., Pacific Exploratory Mission in the tropics: September 1996, *J. Geophys. Res.*, **104**, 5567-5584, 1999.
- Hurst, D. F., D. W. T. Griffith J. N. Carras, D. J. Williams, and P. J. Fraser, Measurements of trace gases emitted by Australian savanna fires during the 1990 dry season, *J. Atmos. Chem.*, **18**, 33-56, 1994.
- Justice, C. O., J. D. Kendall, P. R. Dowty, and R. J. Scholes, Satellite remote sensing of fires during the SAFARI campaign using NOAA advanced very high resolution radiometer data, *J. Geophys. Res.*, **101**, 23,851-23,863, 1996.
- Kok, G. L., S. S. H. Prévôt, R. D. Schillawski, and J. E. Johnson, Carbon monoxide measurements from 76°N to 59°S and over the South Tasman Sea, *J. Geophys. Res.*, **103**, 16,731-16,736, 1998.
- Levine, J. S. (Ed.), *Global Biomass Burning: Atmospheric, Climatic, and Biospheric Implications*, MIT Press, Cambridge, Mass., 1991.
- Levine, J. S. (Ed.), *Biomass Burning and Global Change*, vol. 1 and 2, MIT Press, Cambridge, Mass., 1996.
- Logan, J. A., M. J. Prather, S. C. Wofsy, and M. B. McElroy, Tropospheric chemistry: A global perspective, *J. Geophys. Res.*, **86**, 7210-7254, 1981.
- Matsueda, H., H. Y. Inoue, Y. Sawa, Y. Tsutsumi, and M. Ishii, Carbon monoxide in the upper troposphere over the western Pacific between 1993 and 1996, *J. Geophys. Res.*, **103**, 19,093-19,110, 1998.
- Mauzerall, D. L., et al., Photochemistry in biomass burning plumes and implications for tropospheric ozone over the tropical South Atlantic, *J. Geophys. Res.*, **103**, 8401-8423, 1998.
- Olson, J., B. A. Baum, D. R. Cahoon, and J. H. Crawford, Frequency and distribution of forest, savanna, and crop fires over tropical regions during PEM-Tropics A, *J. Geophys. Res.*, **104**, 5865-5876, 1999.
- Pickering, K. E., et al., Convective transport of biomass burning emissions over Brazil during TRACE-A, *J. Geophys. Res.*, **101**, 23,993-24,012, 1996.
- Sachse, G. W., J. E. Collins Jr., G. F. Hill, L. O. Wade, L. G. Burney, and J. A. Ritter, Airborne tunable diode laser system for high precision concentration and flux measurements of carbon monoxide and methane, *Proc. SPIE Int. Opt. Eng.*, **1433**, 145-156, 1991.
- Sandholm, S. T., et al., Summertime tropospheric observations related to NO_x/O_3 distributions and partitioning over Alaska: Arctic Boundary Layer Expedition 3A, *J. Geophys. Res.*, **97**, 16,481-16,509, 1992.
- Schultz, M. G., et al., On the origin of tropospheric ozone and NO_x over the tropical South Pacific, *J. Geophys. Res.*, **104**, 5829-5844, 1999.
- Seiler, W., and P. J. Crutzen, Estimates of gross and net fluxes of carbon between the biosphere and the atmosphere from biomass burning, *Clim. Change*, **2**, 207-247, 1980.
- Singh, H. B., L. J. Salas, and R. E. Stiles, Methyl halides in and over the eastern Pacific (40°N-32°S), *J. Geophys. Res.*, **88**, 3684-3690, 1983.
- Sive, B. C., Atmospheric NMHCs: Analytical methods and estimated hydroxyl radical concentrations, Ph.D. thesis, Univ. of Calif., Irvine, 1998.
- Smyth, S., et al., Comparison of free tropospheric western Pacific air mass classification schemes for the PEM-West A experiment, *J. Geophys. Res.*, 1743-1762, 1996.
- Talbot, R. W., et al., Chemical characteristics of continental outflow over the tropical South Atlantic Ocean from Brazil and Africa, *J. Geophys. Res.*, **101**, 24,187-24,202, 1996.
- Talbot, R. W., J. E. Dibb, E. M. Scheuer, D. R. Blake, N. J. Blake, G. L. Gregory, G. W. Sachse, J. D. Bradshaw, S. T. Sandholm, and H. B. Singh, Influence of biomass combustion emissions on the distribution of acidic trace gases over the southern Pacific basin during austral springtime, *J. Geophys. Res.*, **104**, 5623-5634, 1999.
- Thompson, A. M., K. E. Pickering, D. P. McNamara, M. R. Schoeberl, R. D. Hudson, J. H. Kim, E. V. Browell, V. W. J. H. Kirchhoff, and D. Nganga, Where did tropospheric ozone over southern Africa and the tropical Atlantic come from in October 1992? Insight from TOMS, GTE TRACE A, and SAFARI 1992, *J. Geophys. Res.*, **101**, 24251-24,279, 1996.
- D. R. Blake, N. J. Blake, J. P. Lopez, L. M. McKenzie, F. S. Rowland, I. J. Simpson, and B. C. Sive, Department of Chemistry, University of California, Irvine, CA, 92697-2025. (e-mail: drblake@uci.edu; nblake@uci.edu; jplopez@uci.edu; rowland@uci.edu; isimpson@uci.edu; bcsive@uci.edu)
- O. W. Wingenter, School of Earth and Atmospheric Sciences, Georgia Institute of Technology, Atlanta, GA 30332. (e-mail: oliver@eas.gatech.edu)
- H. E. Fuelberg, G. L. Gregory, and G. W. Sachse, Department of Meteorology, Florida State University, Tallahassee, FL 32306.
- B. E. Anderson, NASA Langley Research Center, Hampton, VA, 23681.
- G. M. Albercook and M. A. Carroll, Atmospheric, Oceanic and Space Sciences, University of Michigan, Ann Arbor, MI 48109.

(Received August 16, 1998; revised January 7, 1999; accepted February 1, 1999.)